

Discotic liquid crystals of transition metal complexes, 53[†]: Synthesis and mesomorphism of phthalocyanines substituted by *m*-alkoxyphenylthio groups

Yoshiaki Chino^a, Kazuchika Ohta^{*a}, Mutsumi Kimura^b and Mikio Yasutake^c

^aSmart Material Science and Technology, Interdisciplinary Graduate School of Science and Technology, Shinshu University, 1-15-1 Tokida, Ueda, 386-8567, Japan.

^bDivision of Chemistry and Materials, Faculty of Textile Science and Technology, Shinshu University, Ueda 386-8567, Japan

^cComprehensive Analysis Centre for Science, Saitama University, 255 Shimo-okubo, Sakura-ku, Saitama 338-8570, Japan.

Received date (to be automatically inserted after your manuscript is submitted)

Accepted date (to be automatically inserted after your manuscript is accepted)

ABSTRACT: We have successfully synthesised a series of novel octakis(*m*-alkoxyphenylthio)phthalocyaninato copper(II) complexes, (*m*-C_{*n*}OPhS)₈PcCu (*n* = 2, 4, 6, 8, 10, 12, 14, 16: **1b~i**), by our developed method to reveal their mesomorphism. The phase transition behaviour and mesophase structures have been established by using a polarizing optical microscope, a differential scanning calorimeter, and a temperature-dependent small angle X-ray diffractometer. Interestingly, the very short chain-substituted derivatives, (*m*-C₁OPhS)₈PcCu (**1a**) and (*m*-C₂OPhS)₈PcCu (**1b**), show a hexagonal ordered columnar (Col_{h0}) mesophase, whereas each of the other longer-chain-substituted derivatives, (*m*-C_{*n*}OPhS)₈PcCu (*n*=4~16: **1c~i**), shows only rectangular ordered columnar (Col_{r0}) mesophase(s). In contrast to the present longer-chain-substituted *phenylthio* derivatives, each of the previous longer-chain-substituted *phenoxy* derivatives, (*m*-C_{*n*}OPhO)₈PcCu (*n* = 10-20), shows a different columnar mesophase of Col_{h0}. We discuss this difference of mesomorphism from the viewpoint of the different steric hindrance originated by the peripheral substituents, PhO and PhS groups. Moreover, we could estimate the optical band gaps of (*m*-C₁₀OPhO)₈PcCu and (*m*-C₁₀OPhS)₈PcCu (**1f**) from absorption edge of the Q-bands to be 1.79 eV and 1.70 eV, respectively. Therefore, the *phenylthio*-substituted derivative gave a narrower band gap by *ca.* 0.1 eV in comparison with the *phenoxy*-substituted derivative.

KEYWORDS: phthalocyanine, metallomesogen, columnar mesophase, liquid crystals

*Correspondence to: Smart Material Science and Technology, Interdisciplinary Graduate School of Science and Technology, Shinshu University, 1-15-1 Tokida, Ueda, 386-8567, Japan. E-mail: ko52517@shinshu-u.ac.jp; Tel & FAX: +81-268-21-5492.

†Part 52: ref. 45 in this paper.

1. INTRODUCTION

Since the first discotic columnar liquid crystal was found by Chandrasekhar and co-workers in 1977 [1], various discogens have been synthesised up to date. In general, a columnar liquid crystal has a π -conjugated macrocyclic core such as triphenylene, hexabenzocoronene and phthalocyanine (Pc), together with more than six long alkyl chains in the periphery [2]. When these discogens are heated, the peripheral long alkyl chains firstly melt to form soft parts, but the central rigid cores maintain columnar stacking structure due to their strong π - π interaction. Accordingly, columnar liquid crystalline phases can be induced by this special situation. Therefore, pre-melting of the long alkyl chains by heating is driving force to induce liquid crystalline phases. In addition, since π orbitals of the π -conjugated macrocyclic cores are overlapped in one-dimensional columns formed by self-assembly, high charge carrier mobility along the columnar axis may be achieved. Therefore, the columnar liquid crystalline compounds exhibiting high charge carrier mobilities have attracted a lot of our attention to apply to organic semiconducting devices such as organic photovoltaic cell, organic field effect transistor and so on [3]. In our previous works [4-6], we synthesised columnar liquid crystalline phthalocyanine compounds, $(C_{12}H_{25}O)_8PcH_2$ and $(C_{12}H_{25}S)_8PcH_2$, illustrated in Figure 1. The hexagonal ordered columnar (Col_{ho}) phases in $(C_{12}H_{25}O)_8PcH_2$ and $(C_{12}H_{25}S)_8PcH_2$ exhibited high charge carrier mobilities of $0.051\text{ cm}^2/Vs$ and $0.28\text{ cm}^2/Vs$, respectively. Therefore, the *alkylthio*(RS)-substituted phthalocyanine derivative gives about 5 times higher charge carrier mobility than the *alkoxy*(RO)-substituted phthalocyanine derivative. In order to achieve much higher charge carrier mobility in columnar liquid crystalline Pc compounds, the following two points may be furthermore required:

- (1) To show very short intracolumnar stacking distance,
- (2) To exhibit highly ordered alignment (ideally, homeotropic alignment).

In our previous works [7-8], we found that substitution of *m*-alkoxyphenoxy (m - C_nOPhO) groups at the β -positions of Pc gave columnar liquid crystalline derivatives, $(m-C_nOPhO)_8PcCu$ (Figure 1), satisfying above two requirements. Therefore, if we can synthesise columnar liquid crystalline phthalocyanines substituted by *m*-alkoxyphenylthio(m - C_nOPhS) groups instead of *m*-alkoxyphenoxy(m - C_nOPhO) groups, higher charge carrier mobility may be realized. The *alkylthio*-substituted phthalocyanine derivative, $(C_nS)_8PcH_2$, exhibits 5 times higher charge carrier mobility than the *alkoxy*-substituted phthalocyanine derivative, $(C_nO)_8PcH_2$, as mentioned above [4-6]. Therefore, we can expect similarly that the *phenylthio*-substituted derivative, $(PhS)_8PcCu$, may exhibit higher charge carrier mobility than the *phenoxy*-substituted derivative, $(PhO)_8PcCu$. Although the $(PhS)_8PcCu$ derivatives have been reported so far [9-19], no liquid crystalline $(PhS)_8PcCu$ derivatives have been reported.

Recently, we have synthesised $(PhS)_8PcCu$ complexes having very short methoxy groups at the *o*-, *m*-, *m*- & *p*-positions of the phenylthio group to induce mesomorphism in spite of the absence of long alkoxy chains [20]. The thermal fluctuation of the bulky substituents by heating makes soft parts to induce liquid crystalline phases. Hence, they are categorised to “flying-seed-like” liquid crystals [21-25]. However, these flying-seed-like liquid crystals ($x-C_1OPhS$) $_8PcCu$ substituted by very short alkoxy groups are not suitable for application to organic semiconductor, because they show mesomorphism only at extremely high temperatures and transform into isotropic liquid with accompanying decomposition. Therefore, we have planned to synthesise new long *n*-alkoxy-substituted ($m-C_nOPhS$) $_8PcCu$ derivatives showing mesomorphism from room temperature and clearing into isotropic liquid without decomposition.

In this study, we have developed the synthetic route of the new *phenylthio*-substituted derivatives, $(m-C_nOPhS)_8PcCu$ ($n = 2-16$: **1b-1i** in Figure 1), having long *n*-alkoxy groups at the *m*- position, in order to investigate their mesomorphism and mesomorphic structures. In comparison with the previous *phenoxy*-substituted Pc derivatives, $(m-C_nOPhO)_8PcCu$ (n

= 10-20), we discuss the difference of mesomorphism from the viewpoint of the different steric hindrance originated by the peripheral PhO and PhS groups.

2. EXPERIMENTAL

2-1. Materials

The chemical reagents of 3-hydroxybenzenethiol, tritylchloride, Et₃SiH, 3-iodophenol, *n*-alkylbromide, NaBH₄ and 4,5-dichlorophthalonitrile were purchased from Tokyo Chemical Industry and used without further purifications. Other reagents were purchased from Wako Pure Chemical Industries and used without further purifications. Thin layer chromatography sheet (TLC) and silica gel were purchased from Merck. All reaction solvents were purchased from Wako Pure Chemical Industries. DMF was pre-dried over KOH and distilled over CaH₂ under reduced pressure and stored in the presence of 4A molecular sieves. THF was pre-dried over CaCl₂ and distilled from Na wire / benzophenone kethyl. 1-Hexanol was used without further purifications. Deuterated chloroform and DMSO for NMR measurements were purchased from Merck and WAKO Pure Chemical Industries, respectively. Abbreviations of reagents and solvents were as follows:

DBU: 1,8-diazabicyclo[5.4.0]-7-undecene, DMF: *N,N*-dimethylformamide, THF: tetrahydrofuran, DMSO: dimethylsulfoxid and TFA: trifluoroacetic acid

2-2. Measurements

The ¹H-NMR measurements were carried out by using a Bruker Ultrashield 400 M Hz. The MALDI-TOF mass spectral measurements were carried out by using a Bruker Daltonics Autoflex III spectrometer (matrix: dithranol). The elemental analyses were performed by using a Perkin-Elmer Elemental Analyzer 2400. The data of MALDI-TOF mass spectra and elemental analyses are listed in Table 1. Electronic absorption (UV-vis) spectra were recorded by using a Hitachi U-4100 spectrophotometer. UV-vis spectral data of the (*m*-C_nOPhS)₈PcCu complexes synthesised in this study were summarised in Table 2. Thermal gravimetric analysis (TGA) was carried out with a Rigaku Thermo Plus TG8120 thermal gravity analyser. All TGA were performed under N₂ atmosphere. Phase transition behaviour of the present complexes was observed with a polarizing optical microscope (Nikon ECLIPSE E600 POL; magnifications of the objective and ocular lenses were × 10, respectively) equipped with a Mettler FP82HT hot stage and a Mettler FP-90 Central Processor, and a Shimadzu DSC-50 differential scanning calorimeter. The phase transition temperatures and enthalpy changes are listed in Table 3. The mesophases were identified by using a small angle X-ray diffractometer (Bruker Mac SAXS System) equipped with a temperature-variable sample holder adopted a Mettler FP82HT hot stage.

2-3. Synthesis

Schemes 1 and 2 illustrate synthetic routes for the precursors of *m*-alkoxythiophenol (**4b~i**) and the corresponding liquid crystalline Pc derivatives (*m*-C_nOPhS)₈PcCu (**1b~i**), respectively. All reactions were carried out under nitrogen atmosphere.

[Route A]

3-Triphenylmethylsulfanylphenol (2A in Scheme 1)

Synthetic method was adopted that of Ref[26]. A three necked flask dried was charged with 3-hydroxybenzenethiol(1.03 g, 8.15 mmol) and dry pyridine (0.679 g, 8.58 mmol). Trityl chloride(2.27 g, 8.14 mmol) was added to the reaction

mixture and it was stirred at rt for 3.5 hours. When TLC (SiO₂ / AcOEt : *n*-hexane = 1 : 1) confirmed disappearance of the spot of the starting reagent of 3-hydroxybenzenethiol (R_f = 0.50) and appearance of the target compound (R_f = 0.68), the reaction was terminated. The reaction mixture was diluted with water and extracted with dichloromethane. The organic layer was washed with water three times and saturated brine once. The organic layer was collected and dried over Na₂SO₄ overnight. Na₂SO₄ was filtrated off and dichloromethane and pyridine were evaporated *in vacuo*. The residue was dried *in vacuo* to obtain colourless oil (0.268 g). Yield: 85.6%.

¹H-NMR(400 MHz, d₆-DMSO, TMS): δ, ppm 9.31 (brs, 1H, -OH), 7.33-7.20 (m, 15H, ArH), 6.83 (t, *J* = 8.0Hz, 1H, ArH), 6.55-6.52 (m, 1H, ArH), 6.39-6.38 (m, 1H, ArH), 6.32-6.30 (m, 1H, ArH).

1-Decyloxy-3-triphenylmethylsulfanylbenzene (3Af in Scheme 1)

Three necked flask dried was charged with 3-triphenylmethylsulfanylphenol (**2A**: 0.505 g, 1.37 mmol), Cs₂CO₃ (0.564 g, 1.73 mmol) and dry DMF (5 mL) at rt. 1-Bromodecane (0.315 g, 1.42 mmol) was added to the reaction mixture and stirred at rt for 4.5 hours. When TLC (SiO₂ / AcOEt : *n*-hexane = 1 : 1) confirmed disappearance of the spot of starting reagent (R_f = 0.18) of **2A** and appearance of the target compound (**3Af**) (R_f = 0.63), the reaction was terminated. The reaction mixture was diluted with water and extracted with dichloromethane. The organic layer was washed with water three times and saturated brine once. The organic layer was collected and dried over Na₂SO₄ overnight. Na₂SO₄ was filtrated off and dichloromethane was evaporated *in vacuo* to obtain the crude product. It was purified by silica gel column chromatography (R_f = 0.55, CH₂Cl₂ : *n*-hexane = 1 : 2). The solvents were evaporated *in vacuo* and resulting product was dried *in vacuo* to obtain colourless oil (0.598 g). Yield: 85.8%.

¹H-NMR(400 MHz, d₆-DMSO, TMS): δ, ppm 7.35-7.21 (m, 15H, ArH), 6.98 (t, *J* = 7.9Hz, 1H, ArH), 6.71, 6.70 (dd, *J* = 2.4, 6.0Hz, 1H, ArH), 6.59 (d, *J* = 7.8Hz, 1H, ArH), 6.32-6.31 (m, 1H, ArH), 3.58 (t, *J* = 6.6Hz, 2H, -OCH₂-), 1.53 (quin, *J* = 6.4Hz, 2H, -OCCH₂-), 1.32-1.20 (m, 14H, -CH₂- × 7), 0.857 (t, *J* = 6.7Hz, 3H, -CH₃).

3-Decyloxybenzenethiol (4f in Scheme 1)

Synthetic method was adopted that of Ref[27]. A three necked flask was charged with trifluoroacetic acid (3 mL), 1-decyloxy-3-triphenylmethylsulfanylbenzene (**3Af**: 0.598 g, 1.18 mmol), CH₂Cl₂ (1.1 mL) and Et₃SiH(0.487 g, 4.19 mmol). It was stirred at rt for 30 min. The reaction mixture was concentrated *in vacuo* and diluted with water and extracted with dichloromethane. The organic layer was washed with water three times and saturated brine once. The organic layer was collected and dried over Na₂SO₄ overnight. Na₂SO₄ was filtrated off and dichloromethane was evaporated *in vacuo*. Even by using any purification techniques, it was not possible to separate the target compound and the by-compound containing deprotection trityl group.

Therefore, the synthesis of **4f** by Route A was abandoned. Next, synthesis of **4b~i** by Route B in Scheme 1 was carried out.

[Route B]

3-Ethoxyiodobenzene (2Bb in Scheme 1)

A three necked flask dried was charged with K₂CO₃ (1.89 g, 13.7 mmol), 3-iodophenol (1.00 g, 4.55mmol) and dry DMF (5 mL). Ethylbromide(0.595 g, 5.46 mmol) was then added to the reaction mixture and it was stirred at 90 °C. Proceeding of the reaction was monitored by TLC (SiO₂ / *n*-hexane). After one hour, disappearance of the spot of 3-iodophenol (R_f = 0.0) was confirmed, so that the reaction was quenched with water and cooled to rt. The product was extracted with ethyl acetate and the organic layer was washed with water three times and saturated brine once. The organic layer was collected and dried over Na₂SO₄ overnight. Na₂SO₄ was filtrated off and the solvent was evaporated *in vacuo* to obtain yellowish liquid (1.06 g). Yield: 93.8%. The product was used for next reaction without further purification.

¹H-NMR (400MHz, CDCl₃, TMS): δ, ppm 7.27-7.24 (m, 2H, ArH), 6.98 (t, *J* = 8.0Hz, 1H, ArH), 6.86-6.84 (m, *J* = 2.4Hz, 8.4Hz, 1H, ArH), 4.00 (quart, *J* = 6.9Hz, 2H, -OCH₂-), 1.40 (t, *J* = 7.0Hz, 3H, -CH₃).

3-Hexyloxyiodobenzene (2Bd)

Yield: 91.6%. This synthesis was carried out as the same method of **2Bb**. The crude product was purification by silica gel column chromatography (*n*-hexane / R_f = 0.30) to obtain colourless liquid (1.29 g).

¹H-NMR (400MHz, CDCl₃, TMS): δ, ppm 7.20-7.18 (m, 2H, ArH), 6.90 (t, *J* = 7.8Hz, 1H, ArH), 6.79-6.77 (m, 1H, ArH), 3.84 (t, *J* = 6.6Hz, 2H, -OCH₂-), 1.69 (quin, *J* = 7.0Hz, 2H, -OCCH₂-), 1.41-1.22 (m, 6H, -(CH₂)₃-), 0.835 (t, *J* = 7.0Hz, 3H, -CH₃).

¹H-NMR datum was in accordance with that of Ref[28].

Other homologues **2Bc~i** were synthesised by the same method for **2Bd**. Only the yield and ¹H-NMR data were shown below. All compounds were obtained as liquid except for **2Bi**.

3-Butoxyiodobenzene (2Bc)

Yield: 42.7%.

¹H-NMR (400MHz, CDCl₃, TMS): δ, ppm 7.27-7.25 (m, 2H, ArH), 6.98 (t, *J* = 8.0Hz, 1H, ArH), 6.87-6.84 (m, 1H, ArH), 3.92 (t, *J* = 6.4Hz, 2H, -OCH₂-), 1.75 (quin, *J* = 7.0Hz, 2H, -OCCH₂-), 1.48 (sext, *J* = 7.4Hz, 2H, -OCCCH₂-), 0.969 (t, *J* = 7.2Hz, 3H, -CH₃).

3-Octyloxyiodobenzene (2Be)

Yield: 92.2%.

¹H-NMR (400MHz, CDCl₃, TMS): δ, ppm 7.20-7.17 (m, 2H, ArH), 6.91 (t, *J* = 7.8Hz, 1H, ArH), 6.79-6.77 (m, 1H, ArH), 3.84 (t, *J* = 6.6Hz, 2H, -OCH₂-), 1.69 (quin, *J* = 7.2Hz, 2H, -OCCH₂-), 1.40-1.20 (m, 10H, -(CH₂)₅-), 0.818 (t, *J* = 7.0Hz, 3H, -CH₃). The ¹H-NMR datum was in accordance with that of Ref[29].

3-Decyloxyiodobenzene (2Bf)

Yield: 93.9%. ¹H-NMR (400MHz, CDCl₃, TMS): δ, ppm 7.30-7.27 (m, 2H, ArH), 7.04 (t, *J* = 8.2Hz, 1H, ArH), 6.89-6.87 (m, 1H, ArH), 3.97 (t, *J* = 6.4Hz, 2H, -OCH₂-), 1.85 (quin, *J* = 6.6Hz, 2H, -OCCH₂-), 1.50-1.30 (m, 14H, -(CH₂)₇-), 0.946 (t, *J* = 7.0Hz, 3H, -CH₃).

3-Dodecyloxyiodobenzene (2Bg)

Yield: 85.2%. ¹H-NMR (400MHz, CDCl₃, TMS): δ, ppm 7.26-7.24 (m, 2H, ArH), 6.97 (t, *J* = 7.8Hz, 1H, ArH), 6.86-6.83 (m, 1H, ArH), 3.91 (t, *J* = 6.6Hz, 2H, -OCH₂-), 1.75 (quin, *J* = 7.0Hz, 2H, -OCCH₂-), 1.45-1.27 (m, 18H, -(CH₂)₉-), 0.881 (t, *J* = 7.0Hz, 3H, -CH₃).

3-Tetradecyloxyiodobenzene (2Bh)

Yield: 84.1%. ¹H-NMR (400MHz, CDCl₃, TMS): δ, ppm 7.27-7.24 (m, 2H, ArH), 6.97 (t, *J* = 8.0Hz, 1H, ArH), 6.86-6.84 (m, 1H, ArH), 3.91 (t, *J* = 6.4Hz, 2H, -OCH₂-), 1.75 (quin, *J* = 6.6Hz, 2H, -OCCH₂-), 1.47-1.26 (m, 22H, -(CH₂)₁₁-), 0.88 (t, *J* = 7.0Hz, 3H, -CH₃).

3-Hexadecyloxyiodobenzene (2Bi)

Yield: 83.3%. Mp: 32.4 °C. ¹H-NMR(400MH, CDCl₃, TMS): δ, ppm 7.27-7.23 (m, 2H, ArH), 6.98 (t, *J* = 8.0Hz, 1H, ArH), 6.86-6.83 (m, 1H, ArH), 3.91 (t, *J* = 6.6Hz, 2H, -OCH₂-), 1.76 (quin, *J* = 7.0Hz, 2H, -OCCH₂-), 1.43 (quin, *J* = 7.3Hz, 2H, -OCCCH₂-), 1.33-1.26 (m, 24H, -CH₂- × 12), 0.88 (t, *J* = 6.8Hz, 3H, -CH₃).

3-Ethoxybenzenthioi (4b in Scheme 1)

Synthetic method was adopted that of Ref[30]. A three necked flask dried was charged with K₂CO₃(1.00 g, 7.26 mmol), powdered sulfur (0.358 g, 11.2 mmol), CuI (72.3 mg, 0.380 mmol), 3-ethoxyiodobenzene (**2Bb**) (0.897 g, 3.62 mmol) and dry DMF (4 mL). The reaction was carried out at 90 °C with stirring for 12 hours. TLC (SiO₂ / *n*-hexane) confirmed disappearance of the spot of starting reagent of **2Bb** (R_f = 0.30) and appearance of the new spot (R_f = 0.0) were

confirmed by TLC. The reaction mixture was cooled to rt and diluted with water. The product was extracted with ethyl acetate and the organic layer was washed with water three times and saturated brine once. The organic layer was collected and dried over Na₂SO₄ overnight. Na₂SO₄ was filtrated off and the solvent was evaporated *in vacuo* to obtain the crude product, which was used for next reaction without further purification. The three necked flask containing the crude product was charged with NaBH₄(4.24 g, 112 mmol) and dry THF (10 mL) and it was stirred for 32 hours. The reaction was quenched with slowly dropwise adding conc.HCl in an ice bath. The product was extracted with ethyl acetate and the organic layer was washed with water three times and saturated brine once. The organic layer was collected and dried over Na₂SO₄ overnight. Na₂SO₄ was filtrated off and the solvent was evaporated *in vacuo* to obtain colourless liquid (0.382 g). The product was used for next reaction without further purifications. Yield: 68.5%.

¹H-NMR (400MHz, CDCl₃, TMS): δ, ppm 7.12 (t, *J* = 8.0Hz, 1H, ArH), 6.84-6.81 (m, 2H, ArH), 6.68 (dd, *J* = 2.0Hz, 6.0Hz, 1H, ArH), 4.00 (quart, *J* = 7.1Hz, 2H, -OCH₂-), 3.44 (s, 1H, -SH), 1.39 (t, *J* = 7.0Hz, 3H, -CH₃).

Other homologues **4c~i** were synthesised by the same method for **4b**. Only the yield and ¹H-NMR data were shown below. All compounds **4c~i** were obtained as liquid.

3-Butoxybenzenethiol (4c)

Yield: 77.9%.

¹H-NMR (400MHz, CDCl₃, TMS): δ, ppm 7.12 (t, *J* = 8.0Hz, 1H, ArH), 6.84-6.81 (m, 2H, ArH), 6.68 (dd, *J* = 3.2Hz, 7.6Hz, 1H, ArH), 3.93 (t, *J* = 6.4Hz, 2H, -OCH₂-), 3.43 (s, 1H, -SH), 1.75 (quin, *J* = 7.0Hz, 2H, -OCCH₂-), 1.48 (sext, *J* = 7.4Hz, 2H, -OCCCH₂-), 0.969 (t, *J* = 7.4Hz, 3H, -CH₃).

3-Hexyloxybenzenethiol (4d)

Yield: 65.9%.

¹H-NMR (400MHz, CDCl₃, TMS): δ, ppm 7.05 (t, *J* = 7.8Hz, 1H, ArH), 6.76-6.75 (m, 2H, ArH), 6.62-6.60 (m, 1H, ArH), 3.86 (t, *J* = 6.6Hz, 2H, -OCH₂-), 3.36 (s, 1H, -SH), 1.68 (quin, *J* = 7.1Hz, 2H, -OCCH₂-), 1.41-1.27 (m, 6H, -OCCCH₂-), 0.832 (t, *J* = 6.8Hz, 3H, -CH₃).

3-Octyloxybenzenethiol (4e)

Yield: 91.6%.

¹H-NMR (400MHz, CDCl₃, TMS): δ, ppm 7.05 (t, *J* = 8.0Hz, 1H, ArH), 6.76-6.74 (m, 2H, ArH), 6.63-6.60 (m, 1H, ArH), 3.84 (t, *J* = 6.6Hz, 2H, -OCH₂-), 3.36 (s, 1H, -SH), 1.69 (quin, *J* = 7.2Hz, 2H, -OCCH₂-), 1.40-1.22 (m, 10H, CH₂ × 5), 0.816 (t, *J* = 7.0Hz, 3H, -CH₃).

3-Decyloxybenzenethiol (4f)

Yield: 80.5%.

¹H-NMR (400MHz, CDCl₃, TMS): δ, ppm 7.04 (t, *J* = 8.0Hz, 1H, ArH), 6.79-6.73 (m, 2H, ArH), 6.63-6.59 (m, 1H, ArH), 3.84 (t, *J* = 6.6Hz, 2H, -OCH₂-), 3.36 (s, 1H, -SH), 1.75 (quin, *J* = 7.0Hz, 2H, -OCCH₂-), 1.41-1.20 (m, 14H, CH₂ × 7), 0.811 (t, *J* = 6.8Hz, 3H, -CH₃).

3-Dodecyloxybenzenethiol (4g)

Yield: 62.3%.

¹H-NMR (400MHz, CDCl₃, TMS): δ, ppm 7.12 (t, *J* = 8.2Hz, 1H, ArH), 6.84-6.81 (m, 2H, ArH), 6.70-6.67 (m, 1H, ArH), 3.91 (t, *J* = 6.6Hz, 2H, -OCH₂-), 3.43 (s, 1H, -SH), 1.76 (quin, *J* = 7.0Hz, 2H, -OCCH₂-), 1.45-1.27 (m, 18H, CH₂ × 9), 0.881 (t, *J* = 7.0Hz, 3H, -CH₃).

3-Tetradecyloxybenzenethiol (4h)

Yield: 92.7%.

¹H-NMR (400MHz, CDCl₃, TMS): δ, ppm 7.12 (t, *J* = 7.8Hz, 1H, ArH), 6.84-6.81 (m, 2H, ArH), 6.70-6.67 (m, 1H, ArH), 3.92 (t, *J* = 6.6Hz, 2H, -OCH₂-), 3.43 (s, 1H, -SH), 1.76 (quin, *J* = 7.0Hz, 2H, -OCCH₂-), 1.47-1.26 (m, 22H, CH₂ × 11), 0.88 (t, *J* = 6.8Hz, 3H, -CH₃).

3-Hexadecyloxybenzenethiol (4i)

Yield: 51.8%.

¹H-NMR (400MHz, CDCl₃, TMS): δ, ppm 7.12 (t, *J* = 8.2Hz, 1H, ArH), 6.84-6.81 (m, 2H, ArH), 6.69, 6.68 (dd, *J* = 2.0Hz, 6.0Hz, 1H, ArH), 3.92 (t, *J* = 6.6Hz, 2H, -OCH₂-), 3.44 (s, 1H, -SH), 1.76 (quin, *J* = 7.0Hz, 2H, -OCCH₂-), 1.47-1.26 (m, 26H, -(CH₂)₁₃-), 0.88 (t, *J* = 6.4Hz, 3H, -CH₃).

[Route C]

Derivative **4i** was also synthesised by another method of Refs[31-32].

Bis(3-hydroxyphenyl)disulfide (2C in Scheme 1).

In a three neck flask 3-hydroxybenzenethiol(0.247 g, 1.96 mmol) was dissolved in 10 mL of DMSO-CHCl₃ mixed solvent (1 : 1, v/v). To the reaction mixture, 47wt% HBr aq. sol. (72.9 mg, 0.423 mmol) was added and it was stirred at rt for 12.5 hours. When TLC(SiO₂/CHCl₃) confirmed disappearance of the spot of starting reagent of 3-hydroxybenzenethiol (*R_f* = 0.10) and appearance of a new spot of target compound **2C**(*R_f* = 0. 0), the reaction was terminated. The solvents were evaporated *in vacuo* to concentrate the reaction mixture. The product was extracted with ethyl acetate and washed with water three times and saturated brine once. The organic layer was collected and dried over Na₂SO₄ overnight. Na₂SO₄ was filtrated off and the solvent was evaporated *in vacuo*. The residue was dried *in vacuo* to obtain the target compound **2C** as white powder (0.242 g). Yield: 98.5%. Mp: 80-90 °C(broad).

¹H-NMR(400MHz, d₆-DMSO, TMS): δ, ppm 9.75 (s, 2H, -OH), 7.17 (t, *J* = 8.0Hz, 2H, ArH), 6.93-6.90 (m, 4H, ArH), 6.68-6.60 (m, 2H, ArH).

Bis(3-hexadecyloxyphenyl)disulfide (3Ci in Scheme 1)

A three necked flask was charged with bis(3-hydroxyphenyl)disulfide (**2C**) (0.263 g, 1.05 mmol), K₂CO₃ (0.744 g, 5.38 mmol) and dry DMF (4 mL). 1-Bromohexadecane (0.808 g, 2.64 mmol) was then added to the reaction mixture and it was stirred at 90 °C for 3.5 hours. The reaction was terminated when TLC (SiO₂/CH₂Cl₂) confirmed disappearance of both the spots of starting reagent of **2C** (*R_f* = 0.0) and monoalkylated compound (*R_f* = 0.55), and appearance of only one spot of dialkylated compound (SiO₂/CH₂Cl₂, *R_f* = 0.95). The reaction mixture was diluted with water and the product was extracted with dichloromethane. The organic layer was washed with water three times and saturated brine once. The organic layer was collected and dried over Na₂SO₄ overnight. Na₂SO₄ was filtrated off and the solvent was evaporated *in vacuo*. The crude product was recrystallised from acetone and then *n*-hexane at 25 °C to obtain white powder (0.330 g). Yield:44.9%

Mp: 62.5 °C(mp1), 64.8 °C(mp2) (This compound showed double melting behaviour.).

¹H-NMR(400MHz, CDCl₃, TMS): δ, ppm 7.18(t, *J* = 8.2Hz, ArH, 2H), 7.06-7.04(m, ArH, 4H), 6.75, 6.74(dd, *J* = 2.2Hz, 6.6Hz, ArH, 2H), 3.90(t, *J* = 6.6Hz, -(OCH₂)- × 2, 4H), 1.74(quin, *J* = 7.1Hz, -(OCCH₂)- × 2, 4H), 1.45-1.26(m, -(CH₂)- × 26, 52H), 0.879(t, *J* = 6.8Hz, -CH₃ × 2, 6H).

3-Hexadecyloxybenzenethiol (4i in Scheme 1)

Compound **4i** was synthesised from Compound **3Ci** according to the method of Ref[32]. A three necked flask was charged with bis(3-hexadecyloxyphenyl)disulfide (**3Ci**: 0.324 g, 0.464 mmol), PPh₃ (0.299 g, 1.14 mmol) and THF (12 mL) and then conc.HCl aq. sol. (0.4 mL) and H₂O (2mL). It was gently refluxed with stirring for 5 hours. After cooled to rt, large excessive amounts of iodomethane was added to the reaction mixture and stirred at rt for 9 hours. The reaction mixture was diluted with water and extracted with toluene. The organic layer was washed with water three

times and saturated brine once. The organic layer was collected and dried over Na₂SO₄ overnight. Na₂SO₄ was filtrated off and the solvent was concentrated *in vacuo*. *n*-Hexane was added to the solution until precipitation was occurred. It was heated until the precipitates were completely dissolved and then cooled to rt. The resulted precipitates were removed by filtration. To the filtrate *n*-hexane was furthermore added to occur precipitation completely. The precipitates were removed again by filtration, and then the filtrate was evaporated *in vacuo* to remove the solvent to afford colourless oil (0.151 g). Yield: 46.5%.

¹H-NMR (400MHz, CDCl₃, TMS): δ, ppm 7.12 (t, *J* = 8.2Hz, 1H, ArH), 6.84-6.81 (m, 2H, ArH), 6.69, 6.68 (dd, *J* = 2.0Hz, 6.0Hz, 1H, ArH), 3.92 (t, *J* = 6.6Hz, 2H, -OCH₂-), 3.44 (s, 1H, -SH), 1.76 (quin, *J* = 7.0Hz, 2H, -OCCH₂-), 1.47-1.26 (m, 26H, -(CH₂)₁₃-), 0.88 (t, *J* = 6.4Hz, 3H, -CH₃).

[Scheme 2]

4,5-Bis(*m*-ethoxyphenylthio)phthalonitrile (5b)

Synthetic method was adopted that of Ref[33]. A three necked flask was charged with K₂CO₃ (0.653 g, 4.73 mmol), 3-ethoxybenzenethiol (**3a**) (0.234 g, 1.52 mmol) and DMF (5mL) and it was heated up to 90 °C. To the reaction mixture, 4,5-dichlorophthalonitrile (0.102 g, 0.517 mmol) was added and stirred at 90 °C for 7 hours with occasionally monitoring by TLC. When the reaction was completed, it was quenched with water. The product was extracted with ethyl acetate and the organic layer was washed with water three times and saturated brine once. The organic layer was collected and dried over Na₂SO₄ overnight. Na₂SO₄ was filtrated off and the solvent was evaporated *in vacuo*. The crude product was purified by column chromatography (SiO₂, CH₂Cl₂, R_f = 0.50) to obtain white crystals (0.112 g).

Yield: 50.2%. Mp: 139.8 °C.

¹H-NMR (400MHz, CDCl₃, TMS): δ, ppm 7.41 (t, *J* = 8.2Hz, 2H, ArH), 7.12-7.03 (m, 8H, ArH), 4.07 (quart, *J* = 7.1Hz, 4H, -OCH₂-), 1.45ppm(t, *J* = 7.0Hz, 6H, -CH₃).

Other homologues **5c-i** were synthesised by the same method for **5b**. The eluents for the column chromatography, yields, melting points and ¹H-NMR data were described below for these homologues.

4,5-Bis(*m*-butoxyphenylthio)phthalonitrile (5c)

SiO₂, CH₂Cl₂ : *n*-hexane = 4 : 1, R_f = 0.30.

Yield: 68.9%. Mp: 96.1 °C.

¹H-NMR (400MHz, CDCl₃, TMS): δ, ppm 7.41 (t, *J* = 7.4Hz, 2H, ArH), 7.11-7.04 (m, 8H, ArH), 3.99 (t, *J* = 6.6Hz, 4H, -OCH₂-), 1.80 (quin, *J* = 7.0Hz, 4H, -OCCH₂-), 1.51 (sext, *J* = 7.5Hz, 4H, -OCCCH₂-), 0.993 (t, *J* = 7.4Hz, 6H, -CH₃).

4,5-Bis(*m*-hexyloxyphenylthio)phthalonitrile (5d)

SiO₂, CH₂Cl₂ : *n*-hexane = 4 : 1, R_f = 0.48.

Yield: 86.0%. Mp: 64.1 °C.

¹H-NMR (400MHz, CDCl₃, TMS): δ, ppm 7.41 (t, *J* = 7.9Hz, 2H, ArH), 7.11-7.03 (m, 8H, ArH), 3.98 (t, *J* = 6.4Hz, 4H, -OCH₂-), 1.81 (quin, *J* = 7.0Hz, 4H, -OCCH₂-), 1.49-1.33 (m, 12H, (-CH₂)₃ × 2), 0.914 (t, *J* = 7.0Hz, 6H, -CH₃).

4,5-Bis(*m*-octyloxyphenylthio)phthalonitrile (5e)

SiO₂, CH₂Cl₂ : *n*-hexane = 4 : 1, R_f = 0.58.

Yield: 95.1%. Mp: 72.1 °C.

¹H-NMR (400MHz, CDCl₃, TMS): δ, ppm 7.41 (t, *J* = 8.0Hz, 2H, ArH), 7.11-7.03 (m, 8H, ArH), 3.98 (t, *J* = 6.6Hz, 4H, -OCH₂-), 1.81 (quin, *J* = 7.1Hz, 4H, -OCCH₂-), 1.49-1.24 (m, 20H, (-CH₂)₅ × 2), 0.889 (t, *J* = 6.8Hz, 6H, -CH₃).

4,5-Bis(*m*-decyloxyphenylthio)phthalonitrile (5f)

SiO₂, CH₂Cl₂, R_f = 0.80.

Yield: 78.1%. Mp: 76.5 °C.

¹H-NMR (400MHz, CDCl₃, TMS): δ, ppm 7.43 (t, *J* = 7.6Hz, 2H, ArH), 7.13-7.08 (m, 8H, ArH), 4.00 (t, *J* = 6.6Hz, 4H, -OCH₂-), 1.83 (quin, *J* = 7.4Hz, 4H, -OCCH₂-), 1.53-1.31ppm(m, 28H, (-CH₂-)₇ × 2), 0.904 (t, *J* = 6.6Hz, 6H, -CH₃).

4,5-Bis(*m*-dodecyloxyphenylthio)phthalonitrile (5g)

SiO₂, CH₂Cl₂ : *n*-hexane = 4 : 1, R_f = 0.58.

Yield: 29.3%. Mp: 76.2 °C.

¹H-NMR (400MHz, CDCl₃, TMS): δ, ppm 7.41 (t, *J* = 8.2Hz, 2H, ArH), 7.11-7.03 (m, 8H, ArH), 3.98 (t, *J* = 6.6Hz, 4H, -OCH₂-), 1.81 (quin, *J* = 7.1Hz, 4H, -OCCH₂-), 1.50-1.21 (m, 36H, (-CH₂-)₉ × 2), 0.88 (t, *J* = 6.8Hz, 6H, -CH₃).

4,5-Bis(*m*-tetradecyloxyphenylthio)phthalonitrile (5h)

SiO₂, CH₂Cl₂ : *n*-hexane = 4 : 1, R_f = 0.38.

Yield: 75.0%.

Mp: 50.0 °C(mp₁), 83.3 °C(mp₂) (This compound showed double melting behaviour).

¹H-NMR (400MHz, CDCl₃, TMS): δ, ppm 7.41 (t, *J* = 7.8Hz, 2H, ArH), 7.11-7.04 (m, 8H, ArH), 3.98 (t, *J* = 6.4Hz, 4H, -OCH₂-), 1.81 (quin, *J* = 7.0Hz, 4H, -OCCH₂-), 1.49-1.26 (m, 44H, (-CH₂-)₁₁ × 2), 0.879 (t, *J* = 6.8Hz, 6H, -CH₃).

4,5-Bis(*m*-hexadecyloxyphenylthio)phthalonitrile (5i)

SiO₂, CH₂Cl₂ : *n*-hexane = 5 : 2, R_f = 0.70.

Yield: 73.9%.

Mp: 58.3 °C(mp₁), 70.2 °C(mp₂) (This compound showed double melting behaviour.).

¹H-NMR (400MHz, CDCl₃, TMS): δ, ppm 7.41 (t, *J* = 8.2Hz, 2H, ArH), 7.11-7.03 (m, 8H, ArH), 3.98 (t, *J* = 6.4Hz, 4H, -OCH₂-), 1.81 (quin, *J* = 7.0Hz, -OCCH₂-), 1.47 (quin, *J* = 7.2Hz, -OCCCH₂-), 1.38-1.26 (m, 48H, -(CH₂)₁₂-), 0.878 (t, *J* = 6.8Hz, 6H, -CH₃).

Octakis(*m*-ethoxyphenylthio)phthalocyaninato copper(II) (1b)

A three necked flask was charged with anhydrous CuCl₂ (15.5 mg, 0.115 mmol), 4,5-bis(3-ethoxyphenylthio)phthalonitrile (94.1 mg, 0.218mmol) and 1-hexanol (5mL). To the reaction mixture 5 drops of DBU was added and refluxed for 1.5 hours. It was cooled to rt and poured into methanol to precipitate. The precipitates were collected by filtration and washed with methanol, ethanol and ethyl acetate successively. The precipitates were purified by Soxhlet extraction (toluene) two times. The obtained toluene solution was concentrated *in vacuo* and the residue was reprecipitated from acetone to obtain green solid (43.1 mg).

The homologues **1c**, **1h** and **1i** were also synthesised and purified by the same procedure for **1b**.

Octakis(*m*-hexyloxyphenylthio)phthalocyaninato copper(II) (1d)

A three necked flask was charged with anhydrous CuCl₂ (9.2 mg, 0.068 mmol), 4,5-bis(3-hexyloxyphenylthio)phthalonitrile (**5d**: 48.2 mg, 0.0885mmol) and 1-hexanol (5mL). To the reaction mixture 5 drops of DBU was added and it was refluxed with stirring for 1.5 hours. It was cooled to rt and poured into methanol to precipitate. The precipitates were collected by filtration and washed with methanol, ethanol and ethyl acetate successively. The residue was dissolved in chloroform and the solution was concentrated *in vacuo*. Subsequently, the crude product was purified by column chromatography (SiO₂, CHCl₃, R_f = 1.0) to obtain green solid (27.6 mg).

The homologues **1e~g** were also synthesised and purified by the same procedure for **1d**. Table 1 lists the yields, MALDI-TOF-MASS and elemental analysis data of all the homologues **1b~i**. The UV-vis spectral data were summarized in Table 2.

Decomposition temperatures of 1b~1i

Decomposition temperatures (T_d) obtained from TGA are listed below.

1b: $T_d > 400$ °C, **1c:** $T_d = 389$ °C, **1d:** $T_d = 397$ °C, **1e:** $T_d = 359$ °C, **1f:** $T_d = 386$ °C, **1g:** $T_d = 399$ °C, **1h:** $T_d = 371$ °C, **1i:** $T_d = 360$ °C.

3. RESULTS AND DISCUSSION

3-1. Synthesis

Phenylthio substituted phthalocyanine derivatives $(\text{PhS})_8\text{PcM}$ ($M = \text{H}_2$, metal) reported up to date were prepared from commercially available benzenethiol derivatives as the starting reagents[10-20]. However, each of these benzenethiol derivatives doesn't have long alkyl chains. Therefore, at first we have developed the synthetic route for the long alkoxy chain-substituted benzenethiols **4b~i** in this study. Although many synthetic methods for benzenethiol derivatives have been reported so far [34]-[39], we have tried in this study the following three relatively simple methods (Routes A, B and C in Scheme 1) for the long alkoxy chain-substituted benzenethiol precursors **4b-i**.

Route A in Scheme 1 was followed those of Refs[26-27]. The starting material, 3-hydroxybenzenethiol, was commercially available. The thiol group in 3-hydroxybenzenethiol was protected with trityl group to obtain derivative **2A**. Subsequently, the OH group in the phenol derivative **2A** was substituted by an alkoxy group using Williamson reaction to obtain derivative **3Af**. The trityl group in **3Af** was deprotected by triethylsilane in acidic condition. Although the reaction proceeded, it was not possible to separate the target compound **4f** and the by-product containing trityl group. It is attributable to the nonpolarity of both the target compound and the by-product having non-polar decyl groups. In Refs. [26-27], the target benzenethiol derivative can be separated from reaction mixture since substituent R is higher polarity group than decyloxy group. Due to the low polarity of substituent R in this study, Compound **4f** could not be separated from the reaction mixture.

Route B in Scheme 1 was followed that of Ref[30]. Firstly, the OH group in 3-iodophenol was substituted by long alkoxy group using Williamson reaction to obtain derivatives **2Bb~i**. Subsequently, these iodobenzene derivatives **2Bb~i** were successfully converted into benzenethiol derivatives **4b~i** in good yields (average total yield: 62.8%).

Derivative **4i** was also successfully synthesised by using another method [31] (Route C in Scheme 1). Firstly, commercially available 3-hydroxybenzenethiol was converted into corresponding disulfide derivative **2C** in the presence of HBr aq. sol. and DMSO. Subsequently, the OH groups in this disulfide derivative **2C** were substituted by long alkoxy groups using Williamson reaction to obtain disulfide derivative **3Ci**. Following the method of Ref[32], derivative **3Ci** was converted into corresponding benzenethiol derivative **4i**. This method also successfully provided the key benzenethiol derivative **4i** in moderate yield (total yield: 20.1%).

Thus, the methods of Routes B and C in Scheme 1 successfully provided the long alkoxy-substituted benzenethiol derivatives **4b~i**.

As shown in Scheme 2, the synthetic method of target phthalocyanine derivatives $(m\text{-C}_n\text{OPhS})_8\text{PcCu}$ (**1a~i**) was followed the method of Ref[33]. Firstly, each of the long alkoxy-substituted benzenethiol derivatives **4a~i** was reacted with 4,5-dichlorophthalonitrile to obtain the phthalonitrile derivatives **5a~i**. These phenylthio-substituted phthalonitriles **5a~i** were tetracyclised to afford the target phenylthio-substituted phthalocyanines, $(m\text{-C}_n\text{OPhS})_8\text{PcCu}$ (**1a~i**), in relatively good yields (average yield: 59%). Each of the phthalocyanines could be satisfactorily identified by the MALDI-TOF MASS, elemental analysis and UV-vis spectrum (Tables 1 and 2).

3-2. Phase transition behaviour

Table 3 summarizes phase transition behaviour of all the phenylthio-substituted PcCu complexes: the shortest-alkoxy-substituted derivative ($m\text{-C}_1\text{OPhS}$)₈PcCu (**1a**) synthesised in our previous work, and the other longer-alkoxy-substituted derivatives, ($m\text{-C}_n\text{OPhS}$)₈PcCu ($n = 2\sim 16$; **1b~i**), synthesised in this work.

In Figure 2, the phase transition temperatures of all the derivatives ($m\text{-C}_n\text{OPhS}$)₈PcCu ($n = 1\sim 16$; **1a~i**) were plotted against the alkyl chain length (n). As can be seen this figure, each of the lines for the clearing points (\circ), the highest melting points (\bullet), and the liquid crystal - liquid crystal transition points (\blacktriangle) is very smoothly connected. However, there is only a gap between $n = 2$ and 4 for the melting points. It may correspond to the difference of mesomorphism driving forces between the hexagonal ordered columnar (Col_{ho}) phases for **1a-b** ($n = 1, 2$) and the rectangular ordered columnar (Col_{ro} (P2m)) phases for **1c~i** ($n = 4\sim 16$). Furthermore, each of the derivatives **1f~i** ($n = 10\sim 16$) shows two rectangular ordered columnar phases of Col_{ro1} (P2m) and Col_{ro2} (P2m).

Interestingly, the Col_{ho} phases appear only for the extremely short alkoxy-substituted derivatives **1a-b** ($n = 1, 2$), so that these discogens can be considered as flying-seed-like liquid crystals induced by thermal fluctuation of the bulky peripheral substituents [20-25]. On the other hand, the Col_{ro} (P2m) phase(s) appear only for the longer alkoxy-substituted derivatives **1c~i** ($n = 4\sim 16$), so that these discogens can be considered as conventional liquid crystals induced by melting of the peripheral long alkoxy chains. To our best our knowledge, this is the first example changing from flying-seed-like liquid crystals to long alkyl chain type of liquid crystals in a series of liquid crystalline homologues.

3-3. Polarizing optical microscopic observation

Figure 3 shows the polarizing optical photomicrographs of liquid crystalline phases in the representative derivatives, **1b** ($n = 2$), **1f** ($n = 10$) and **1i** ($n = 16$). Both (A) and (B) are the photomicrographs of the liquid crystalline phase in the shortest alkoxy-substituted derivative ($m\text{-C}_2\text{OPhS}$)₈PcCu (**1b**) at 220 °C. As can be seen from these photos, photo (A) shows a focal conic texture typical of liquid crystalline phases and photo (B) shows a dendritic texture typical of a hexagonal columnar (Col_{h}) phase. Therefore, this liquid crystalline phase of **1b** could be identified as a Col_{h} phase. Photo (C) is a Col_{ro2} (P2m) phase in the moderately long alkyl-substituted derivative ($m\text{-C}_{10}\text{OPhS}$)₈PcCu (**1f**) at 115 °C. Both (D) and (E) are a Col_{ro1} (P2m) phase in the same derivative **1f** at 90 °C. As can be seen from these photos, both $\text{Col}_{\text{ro1,2}}$ phases did not give any typical textures of mesophases. However, when the phase in photo (D) was pressed and sheared, it showed both stickiness and birefringence as shown in photo (E). Therefore, the Col_{ro1} (P2m) phase in **1f** could be identified as a liquid crystalline phase. Photo (F) shows a Col_{ro1} (p2m) phase in the longest alkoxy-substituted derivative ($m\text{-C}_{16}\text{OPhS}$)₈PcCu (**1i**) at 100 °C. This photo exhibits a focal conic texture typical of liquid crystalline phases. In addition, when this sample was pressed and sheared, it showed both stickiness and birefringence as shown in photo (G). Therefore, this phase could be also identified as a liquid crystalline phase.

3-4. Temperature-dependent small angle X-ray diffraction (TD-SAXS) measurements

Table 4 summarizes temperature-dependent small angle X-ray diffraction (TD-SAXS) data of the liquid crystalline phases in ($m\text{-C}_n\text{OPhS}$)₈PcCu (**1a~i**). Figures 4, 5 and 6 show the representative SAXS patterns of ($m\text{-C}_2\text{OPhS}$)₈PcCu (**1b**), ($m\text{-C}_{10}\text{OPhS}$)₈PcCu (**1f**) and ($m\text{-C}_{16}\text{OPhS}$)₈PcCu (**1i**), respectively. In these figures, the enlarged diffractograms are shown as the insets. These SAXS patterns were measured for the samples obtained by cooling from isotropic liquid.

The SAXS pattern of ($m\text{-C}_2\text{OPhS}$)₈PcCu (**1b**) at 220 °C is shown in Figure 4. As can be seen from this figure, a very broad halo (#1) due to thermal fluctuation of phenylthio groups was observed in $2\theta = 13\sim 23^\circ$. This broad halo #1 was also observed for the previous flying-seed-like liquid crystalline derivative, ($m\text{-C}_1\text{OPhS}$)₈PcCu (**1a**) [20]. The d-spacings in the low angle region are in a ratio of $1 : 1/\sqrt{3} : 1/\sqrt{7} : 1/3$, which is typical of a Col_{h} phase. Therefore, the mesophase could be identified as a Col_{h} phase. This identification is consistent with the dendritic texture typical of a Col_{h}

mesophase mentioned above. In addition, two peaks at around $2\Theta = 6^\circ$ and 13° could be assigned to the interdimer stacking $d_{001}(2h = 14.3\text{\AA})$ and the intermonomer stacking $d_{001}(h = 7.12\text{\AA})$, respectively. This means that an equilibrium between the dimers and monomers exists in the Col_{ho} mesophase as the same case as the $[\text{m},p\text{-}(\text{C}_n\text{O})_2\text{PhO}]_8\text{PcCu}$ derivatives reported in 2001 [7]. From the Z value calculation [40], the Z value of this Col_{ho} mesophase in **1b** could be obtained as $Z = 1.0$ assuming the intermonomer stacking distance as $h = 7.12\text{\AA}$ and the density of the mesophase as $\rho = 1.0\text{ g}\cdot\text{cm}^{-3}$. Although the intracolumnar stacking distance h (7.12\AA) is much larger than that of conventional Col_{ho} phases. However, the value $Z = 1.0$ is consistent with the theoretical value ($Z = 1.0$) for a Col_{ho} mesophase. Moreover, the large stacking distance $h = 7.12\text{\AA}$ is comparable as that of flying-seed-like liquid crystals reported in our previous works [20, 24]. Thus, the present derivative **1b** could be classified as a flying-seed-like liquid crystal similar to the previously reported derivative **1a**. In our previous work, this liquid crystalline phase of **1a** was identified as a $\text{Col}_{\text{ro}}(\text{P2m})$ phase [20]. However, the d spacings of **1a** are also in a ratio of $1 : 1/\sqrt{3} : 1/\sqrt{7} : 1/3$ as the same as that of **1b**. From the Z value calculation, the result ($Z = 0.95 \doteq 1.0$) is consistent with a Col_{ho} phase. Moreover, the equilibrium between the dimers and monomers in the Col_{ho} mesophase could be also observed as the same case as the $(\text{m}\text{-}\text{C}_2\text{OPhS})_8\text{PcCu}$ (**1b**) homologue. Therefore, the liquid crystalline phase of **1a** could be also identified as Col_{ho} phase, so that we correct the identification of this mesophase from $\text{Col}_{\text{ro}}(\text{P2m})$ to Col_{ho} in this study.

Figure 5 shows a SAXS pattern of the moderately long alkoxy-substituted derivative $(\text{m}\text{-}\text{C}_{10}\text{OPhS})_8\text{PcCu}$ (**1f**) at 115°C . As can see from this figure, a broad halo (#2) due to the molten long alkyl chains was observed. From the reciprocal lattice calculation [40], the liquid crystalline phase was identified as $\text{Col}_{\text{ro2}}(\text{P2m})$ ($a = 37.0\text{ \AA}$, $b = 27.6\text{ \AA}$, $h = 4.06\text{ \AA}$). Figure 6 shows the SAXS pattern of the longest alkoxy-substituted derivative $(\text{m}\text{-}\text{C}_{16}\text{OPhS})_8\text{PcCu}$ (**1i**) at 100°C . The liquid crystalline phase was also identified as $\text{Col}_{\text{ro1}}(\text{P2m})$ ($a = 49.9\text{ \AA}$, $b = 28.6\text{ \AA}$, $h = 4.07\text{ \AA}$). It is very interesting that each of the present longer alkoxy-substituted *phenylthio* derivatives $(\text{m}\text{-}\text{C}_n\text{OPhS})_8\text{PcCu}$ ($n = 4\sim 16$) showed only *rectangular* columnar ($\text{Col}_{\text{ro}}(\text{P2m})$) phase(s), whereas each of the previous longer alkoxy-substituted *phenoxy* derivatives $(\text{m}\text{-}\text{C}_n\text{OPhO})_8\text{PcCu}$ ($n = 10\sim 20$) showed only a *hexagonal* columnar (Col_{ho}) phase [8-9].

3-5. Columnar stacking structures of $(\text{m}\text{-}\text{C}_n\text{OPhO})_8\text{PcCu}$ ($n = 10\text{-}20$) and $(\text{m}\text{-}\text{C}_n\text{OPhS})_8\text{PcCu}$ ($n = 1\text{-}16$).

The different mesophase appearance mentioned above may be attributed to difference of interaction among the Pc cores having steric hindrance of the peripheral substituents (PhO and PhS).

It is well known that stronger interaction between cores is required to form a rectangular columnar (Col_{r}) phase in comparison with a hexagonal columnar (Col_{h}) phase [41-43]. As schematically shown in Figure 7, covalent bond radius of sulfur atom (1.04 \AA) is larger than that of oxygen atom (0.66 \AA). Hence, C-S bond length (1.81 \AA) is longer than C-O bond length (1.43 \AA) [44]. Accordingly, the interaction between Pc cores in the *phenoxy*-substituted derivatives $(\text{m}\text{-}\text{C}_n\text{OPhO})_8\text{PcCu}$ ($n = 10\text{-}20$) is weakened by bigger steric hindrance of the *phenoxy* groups closer to the Pc core. As the result, the *phenoxy*-substituted derivatives $(\text{m}\text{-}\text{C}_n\text{OPhO})_8\text{PcCu}$ ($n = 10\text{-}20$) may form the hexagonal columnar phase (Col_{h}). On the other hand, the interaction between Pc cores in the *phenylthio*-substituted derivatives $(\text{m}\text{-}\text{C}_n\text{OPhS})_8\text{PcCu}$ ($n = 4\text{-}16$) is strengthened by smaller steric hindrance of phenylthio group farther from the Pc core. In this case, an additional coordination bonds may be formed between copper atoms and nitrogen atoms between the upper and lower Pc cores, as illustrated in Figure 7 (dotted lines). Thus, the *phenylthio*-substituted derivatives $(\text{m}\text{-}\text{C}_n\text{OPhS})_8\text{PcCu}$ ($n = 4\text{-}16$) may form the rectangular columnar (Col_{r}) phase.

3-6. UV-vis absorption spectra

Figure 8 shows the UV-vis absorption spectra of $(\text{m}\text{-}\text{C}_{10}\text{OPhO})_8\text{PcCu}$ (upper) and $(\text{m}\text{-}\text{C}_{10}\text{OPhS})_8\text{PcCu}$ (**1f**) (lower) in THF solution. Table 5 lists their spectral data. As can see from these figure and table, the Q-band of the *phenylthio*-

substituted derivative (m -C₁₀OPhS)₈PcCu (**1f**) red-shifts by 35.7 nm into near infrared region compared with the *phenoxy*-substituted derivative (m -C₁₀OPhO)₈PcCu. This result is compatible with those of the *phenylthio*-substituted phthalocyanines reported so far [16-20].

Moreover, we could estimate the optical band gaps of (m -C₁₀OPhO)₈PcCu and (m -C₁₀OPhS)₈PcCu (**1f**) from absorption edge of the Q-bands to be 1.79 eV and 1.70 eV, respectively. Hence, the *phenylthio*-substituted derivative gave a narrower band gap by *ca.* 0.1 eV in comparison with the *phenoxy*-substituted derivative.

3. CONCLUSION

In this study, we have successfully synthesised novel phenylthio-substituted phthalocyanine derivatives (m -C_nOPhS)₈PcCu (**1b~i**) to reveal their mesomorphism. We found that the shortest alkoxy-substituted derivatives, (m -C₁OPhS)₈PcCu (**1a**) and (m -C₂OPhS)₈PcCu (**1b**) could be classified as flying-seed-like liquid crystals. On the other hand, the other longer alkoxy-substituted derivatives (m -C_nOPhS)₈PcCu: n = 4~16 (**1c~i**) could be classified as conventional long alkyl-chain-melting liquid crystals. It is very interesting that each of the present longer alkoxy-substituted *phenylthio* derivatives (m -C_nOPhS)₈PcCu (n = 4~16) showed only *rectangular* columnar (CoI_{r0}(P2m)) phase(s), whereas each of the previous longer alkoxy-substituted *phenoxy* derivatives (m -C_nOPhO)₈PcCu (n = 10~20) showed only a *hexagonal* columnar (CoI_{h0}) phase. The different mesophase appearance may be originated from the difference of interaction among the Pc cores having steric hindrance of the peripheral substituents (PhO and PhS). The Q-band of the *phenylthio*-substituted derivative (m -C₁₀OPhS)₈PcCu (**1f**) red-shifts by 35.7 nm into near infrared region compared with the *phenoxy*-substituted derivative (m -C₁₀OPhO)₈PcCu. Thus, in this study, we successfully synthesised a novel series of liquid crystalline (m -C_nOPhS)₈PcCu (n = 1~16) derivatives showing the Q-bands in near infrared region. We intend to measure the charge carrier mobilities in the near future.

REFERENCES

1. Chandrasekhar S, Sadashira BK, Suresh KA, *Pramana* 1977; **9**: 471-480.
2. Cammidge AN, Bushby RJ, Handbook of Liquid Crystals vol.2B, ch.7, Wiley-VCH: 1998; 693-743.
3. Sergeev S, Pisula W, Geerts YH, *Chem.Soc.Rev.* 2007; **36**: 1902-1929.
4. Ban K, Nishizawa K, Ohta K, Shirai H, *J.Mater.Chem* 2000; **10**: 1083-1090.
5. van de Craats AM, Shouten PG, Warman JM, *Ekisho*, 1998; Vol. 2, No.1.
6. Warman JM, Kroeze JE, Schouten PG, van de Craats AM *J.Porphyrins Phthalocyanines* 2003; **7**: 342-350.
7. Hatsusaka K, Ohta K, Yamamoto I, Shirai H, *J.Mater.Chem* 2001; **11**: 423-433.
8. Ichihara M, Suzuki A, Hatsusaka K, Ohta K, *J.Porphyrins Phthalocyanines* 2007; **11**: 503-512.
9. Sato H, Igarashi K, Yama Y, Ichihara M, Itoh E, Ohta K, *J.Porphyrins Phthalocyanines* 2012; **16**: 1148-1158.
10. Kandaz M, Yilmaz İ, Bekarog˘lu Ö, *Polyhedron* 2000; **19**: 115-121.
11. Balakireva OV, Maizlish VE, Shaposhnikov GP, *Russ.J.Gen.Chem.* 2003; **73**: 292-296.
12. Kobayashi N, Ogata H, Nonaka N, Luk'yanets EA, *Chem.Eur.J.* 2003; **9**: 5123-5134.
13. Lu G, Bai M, Li R, Zhang X, Ma C, Lo P-C, Ng DKP, Jiang J, *Eur.J.Inorg.Chem.* 2006; 3703-3709.
14. Arican D, Arici M, Uğur AL, Erdoğmus A, Koca A, *Electrochimica Acta* 2013; **106**: 541-555.
15. Mayukh M, Lu C-W, Hernandez E, McGrath DV, *Chem.Eur.J.* 2011; **17**: 8427-8478.
16. Polaske NW, Lin H-C, Tang A, Mayukh M, Oquendo LE, Green J, Ratcliff EL, Armstrong NR, Saavedra SS, McGrath DV, *Langmuir* 2011; **27**: 14900-14909.
17. Yu L, Shi W, Lin L, Guo Y, Li R, Peng T, *Dyes and Pigments* 2015; **114**: 231-238.

18. Shi W, Peng B, Guo Y, Lin L, Peng T, Li R, *J.Photochem.Photobio.A:Chemistry* 2016; **321**: 248-256.
19. Zimcik P, Malkova A, Hrubá L, Miletin M, Novakova V, *Dyes and Pigments* 2017; **136**: 715-723.
20. Ishikawa A, Ohta K, Yasutake M, *J.Porphyrins Phthalocyanines* 2015; **19**: 639-650.
21. Ohta K, Shibuya T, Ando M, *J.Mater.Chem.* 2006; **16**: 3635-3639.
22. Takagi Y, Ohta K, Shimosugi S, Fujii T, Itoh E, *J.Mater.Chem.* 2012; **22**: 14418-14425.
23. Hachisuga A, Yoshioka M, Ohta M, Itaya T, *J.Mater.Chem.C.* 2013; **1**: 5315-5321.
24. Yoshioka M, Ohta K, Yasutake M, *RSC.Adv.*, 2015; **5**: 13828-13839.
25. Watarai A, Ohta K, Yasutake M, *J.Porphyrins Phthalocyanines*, 2016; **20**: 822-832.
26. Barluenga S, Dakas P-Y, Ferandin Y, Meijer L, Winssinger N, *Angew.Chem.Int.Ed.* 2006; **45**: 3951-3954.
27. Patent PCT/US2006/041501
28. Hwang JY, Arnold LA, Zhu F, Kosinski A, J.Mangano T, Setola V, Roth BL, Guy RK, *J.Med.Chem.* 2009; **52**: 3892-3901.
29. Wakioka M, Ikegami M, Ozawa F, *Macromolecules*, 2010; **43**: 6980-6985.
30. Jiang Y, Qin Y, Xie S, Zhang X, Dong J, Ma D, *Org.Lett.*, 2009; **11**: 5250-5253.
31. Natarajan P, Sharma H, Kaur M, Sharma P, *Tetrahedron.Lett.*, 2015; **56**:5578-5582.
32. Patel SK, Long TE, *Tetrahedron.Lett.*, 2009; **50**: 5067-5070.
33. Wöhrle D, Eskes M, Shigehara K, Yamada A, *Synthesis*, 1993; 194-196.
34. Kamiyama T, Enomoto S, Inoue M, *Chem.Pharm.Bull.*, 1985; **33**: 5184-5189.
35. Newman MS, Karnes HA, *J.Org.Chem.*, 1996; **31**: 3980-3984.
36. Itoh T, Mase T, *Org.Lett.*, 2004; **6**: 4587-4590.
37. Itoh T, Mase T, *J.Org.Chem.*, 2006; **71**: 2203-2206.
38. Mazzi KA, Okamoto K, Li Z, Gutmann S, Strein E, Glinger DS, Sclaf R, Luscombe CK *Chem.Commun.*, 2013; **49**: 1321-1323.
39. Heine NB, Studer A, *Macromol.Rapid.Commun.*, 2016; **37**: 1494-1498.
40. Ohta K. "Dimensionality and Hierarchy of Liquid Crystalline Phases: X-ray Structural Analysis of the Dimensional Assemblies", Shinshu University Institutional Repository, submitted on 11 May, 2013; <http://hdl.handle.net/10091/17016>; Ohta K. "Identification of discotic mesophases by X-ray structure analysis," in "Introduction to Experiments in Liquid Crystal Science (Ekisho Kagaku Jikken Nyumon [in Japanese])," ed., Japanese Liquid Crystal Society, Chapter 2-(3), pp. 11-21, Sigma Shuppan, Tokyo, 2007; ISBN-13: 978-4915666490.
41. Laschat S, Baro A, Steinke N, Giesselmann F, Hägele C, Scalia G, Judele R, Kapatsina E, Sauer S, Schreivogel A, Tosoni M *Angew.Chem.Int.Ed.*, 2007; **46**: 4832-4887.
42. Zheng H, Lai CK, Swager TM *Chem.Mater.*, 1995; **7**: 2067-2077.
43. Morale F, Date RW, Gullion D, Bruce DW, Finn RL, Wilson C, Blake AJ, Schröder M, Donnio B *Chem.Eur.J.*, 2003; **9**: 2484-2501.
44. Atkins PW, de Paula J *Physical Chemistry*, eight edition, 2006.
45. Watarai A, Ohta K, Yasutake M, *J. Porphyrins Phthalocyanines*, 2016; **20**: 1444-1456.

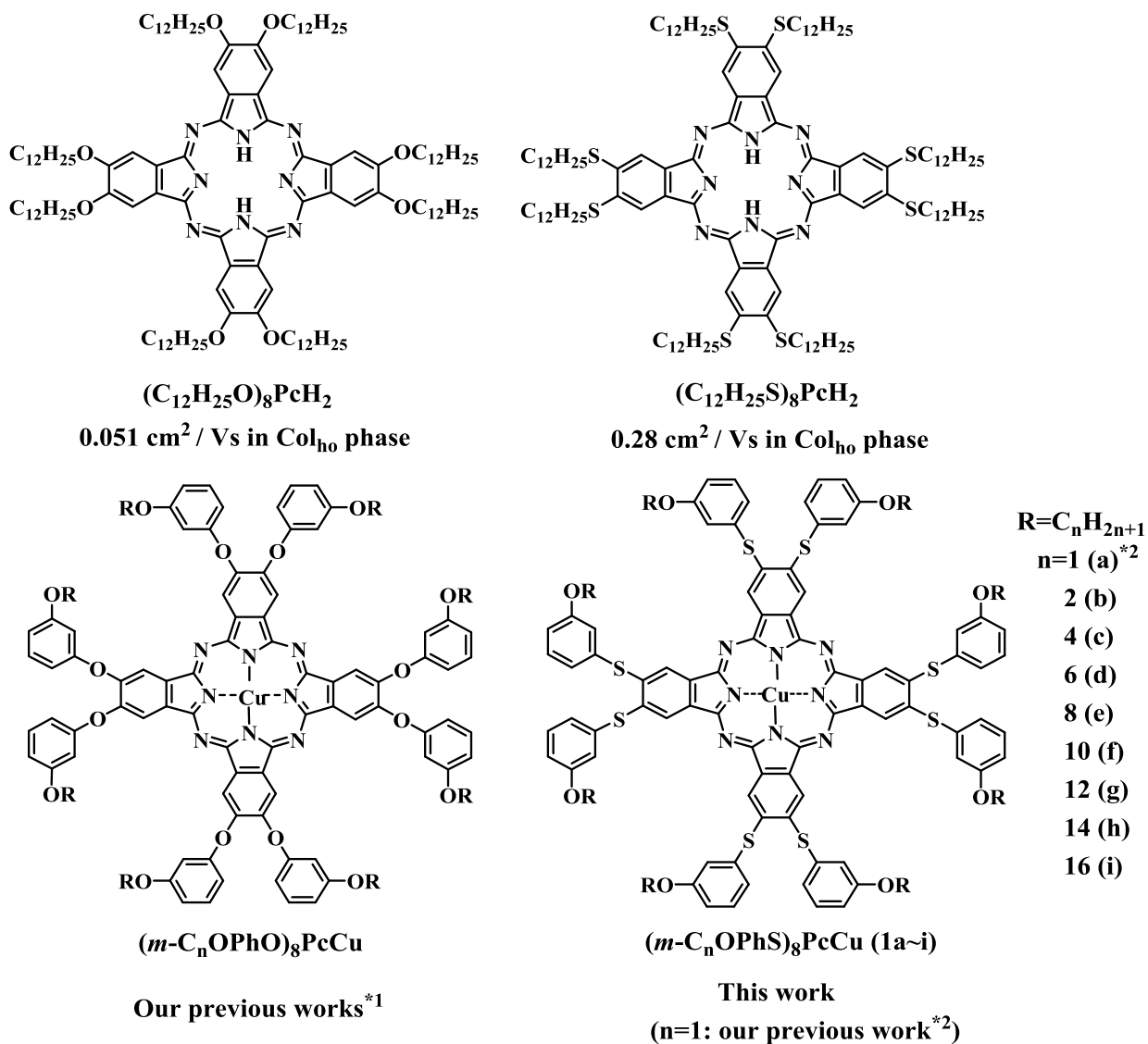
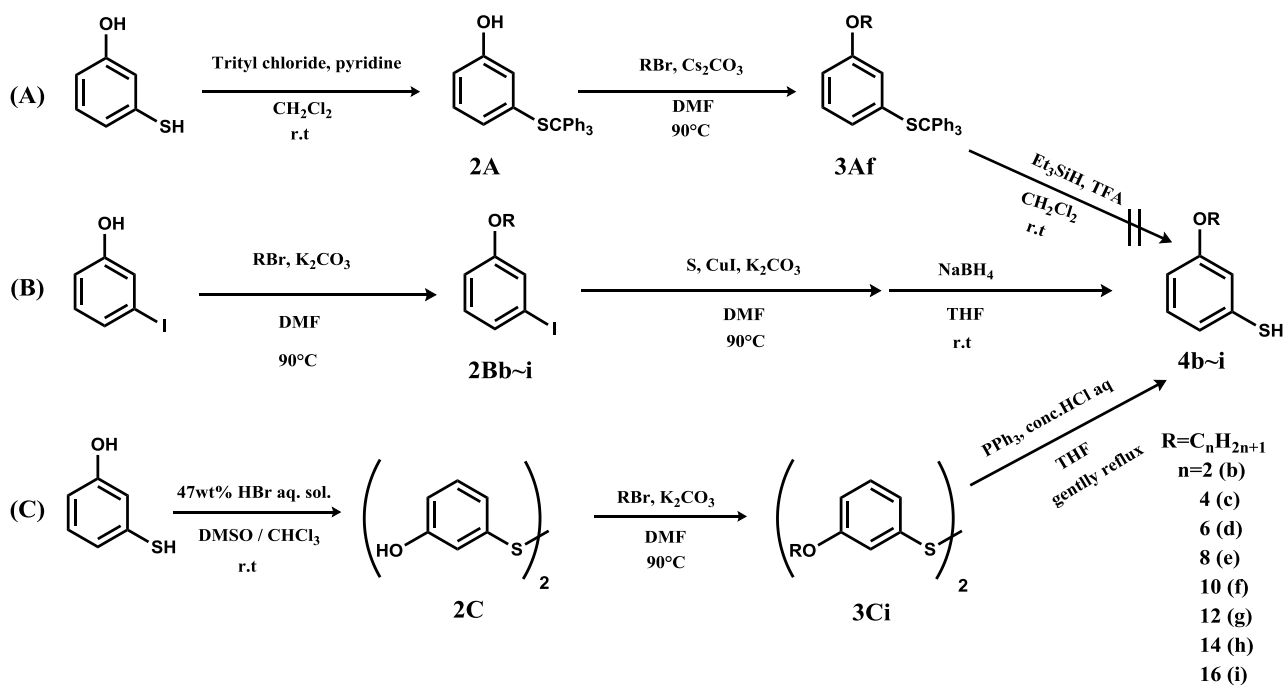
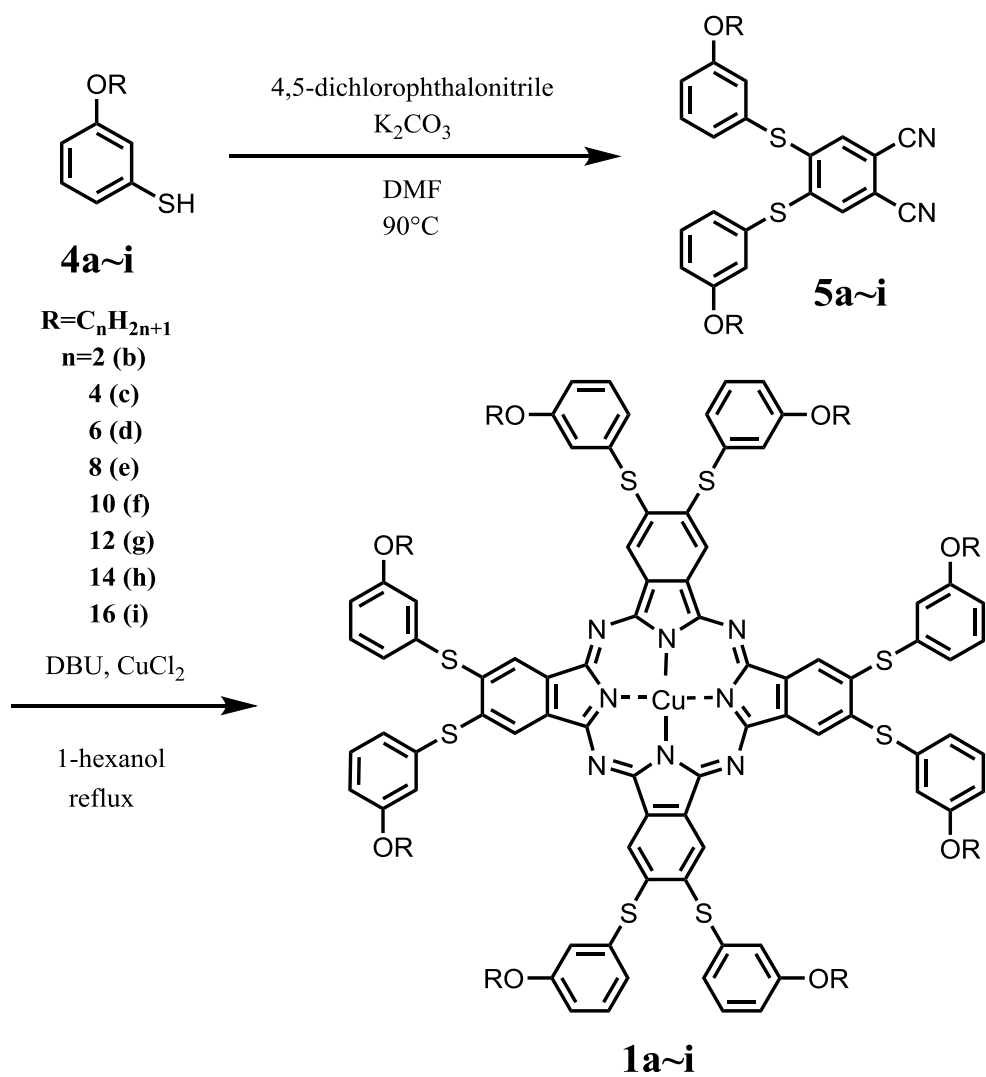


Fig 1. Molecular formulae of liquid crystals based on phthalocyanine. *1: Refs.: [8], [9] and [21]. *2: Ref.: [20].



Scheme 1. Synthetic routes **A**, **B** and **C** for 3-alkoxybenzenethiol: (A) by using the methods adopted Refs. [26] and [27]; (B) Ref. [30]; (C) Ref. [31].



Scheme 2. Synthetic route for $(m\text{-C}_n\text{OPhS})_8\text{PcCu}$ (**1a~i**) · : Previous work (Ref.[20]).

Table 1. Yields and elemental analysis data of (*m*-C_nOPhS)₈PcCu (**1a~i**).

Compound	Mol. formula (Mol. wt)	Exact Mass	Mass observed	Elemental analysis: Found(Calcd.)(%)			Yield(%)
				C	H	N	
1b: (<i>m</i> -C ₂ OPhS) ₈ PcCu	C ₉₆ H ₈₀ N ₈ O ₈ S ₈ Cu (1793.77)	1791.32	1791.32	64.60 (64.28)	4.91 (4.50)	5.92 (6.25)	44.1
1c: (<i>m</i> -C ₄ OPhS) ₈ PcCu	C ₁₁₂ H ₁₁₂ N ₈ O ₈ S ₈ Cu (2018.21)	2015.58	2015.50	66.30 (66.65)	5.74 (5.59)	5.47 (5.55)	65.9
1d: (<i>m</i> -C ₆ OPhS) ₈ PcCu	C ₁₂₈ H ₁₄₄ N ₈ O ₈ S ₈ Cu (2242.64)	2239.83	2239.80	68.69 (68.55)	6.57 (6.47)	5.05 (5.00)	55.7
1e: (<i>m</i> -C ₈ OPhS) ₈ PcCu	C ₁₄₄ H ₁₇₆ N ₈ O ₈ S ₈ Cu (2467.06)	2467.06	2464.14	69.97 (70.11)	7.31 (7.19)	4.81 (4.54)	60.4
1f: (<i>m</i> -C ₁₀ OPhS) ₈ PcCu	C ₁₆₀ H ₂₀₈ N ₈ O ₈ S ₈ Cu (2691.49)	2688.33	2688.31	71.76 (71.40)	8.10 (7.79)	4.22 (4.16)	65.6
1g: (<i>m</i> -C ₁₂ OPhS) ₈ PcCu	C ₁₇₆ H ₂₄₀ N ₈ O ₈ S ₈ Cu (2915.91)	2912.58	2913.61	72.47 (72.49)	8.53 (8.30)	3.59 (3.84)	68.1
1h: (<i>m</i> -C ₁₄ OPhS) ₈ PcCu	C ₁₉₂ H ₂₇₂ N ₈ O ₈ S ₈ Cu (3140.34)	3136.83	3138.02	73.34 (73.43)	8.92 (8.73)	3.55 (3.57)	47.4
1i: (<i>m</i> -C ₁₆ OPhS) ₈ PcCu	C ₂₀₈ H ₃₀₄ N ₈ O ₈ S ₈ Cu (3364.79)	3361.07	3362.24	74.07 (74.25)	9.42 (9.11)	3.23 (3.33)	66.1

Table 2. UV-vis spectral data in CHCl₃ solution of (*m*-C_nOPhO)₈PcCu (**1b~i**).

Compound	Concentration (X10 ⁻⁶ mol L ⁻¹)	λ / nm (logε)		
		Soret band	Q-band	
			Q ₀₋₁ -band	Q ₀₋₀ -band
1b: (<i>m</i> -C ₂ OPhS) ₈ PcCu	2.32	344.0(4.91)	642.0(4.68)	718.0(5.42)
1c: (<i>m</i> -C ₄ OPhS) ₈ PcCu	2.39	344.0(4.92)	642.0(4.69)	716.0(5.42)
1d: (<i>m</i> -C ₆ OPhS) ₈ PcCu	2.26	344.0(4.93)	642.0(4.69)	718.0(5.43)
1e: (<i>m</i> -C ₈ OPhS) ₈ PcCu	2.26	344.0(4.93)	642.0(4.70)	718.0(5.44)
1f: (<i>m</i> -C ₁₀ OPhS) ₈ PcCu	2.29	345.5(4.90)	643.0(4.65)	718.9(5.42)
1g: (<i>m</i> -C ₁₂ OPhS) ₈ PcCu	2.42	342.0(4.88)	642.0(4.66)	718.0(5.40)
1h: (<i>m</i> -C ₁₄ OPhS) ₈ PcCu	2.34	344.0(4.88)	642.0(4.65)	718.0(5.38)
1i: (<i>m</i> -C ₁₆ OPhS) ₈ PcCu	2.37	344.0(4.89)	642.0(4.65)	718.0(5.38)

Table 3. Phase transition temperatures and enthalpy changes of **1a~i**.

Compound	Phase	T (°C) [ΔH (kJmol ⁻¹)]	Phase	Relaxation
1a* : (<i>m</i> -C ₁ OPhS) ₈ PcCu	K ₁	ca. 180	K ₂	
			Col _{ho}	334.2[6.7] → I.L. (decomp.)
1b : (<i>m</i> -C ₂ OPhS) ₈ PcCu			K _v	212.5[57.6] ← Col _{ho} → 239.5[6.1] → I.L.
1c : (<i>m</i> -C ₄ OPhS) ₈ PcCu			K _v	191.3 → Col _{ro2} (P2m) ← 199.9 → I.L.
1d : (<i>m</i> -C ₆ OPhS) ₈ PcCu	K _{1v}	95.0[7.2]	K ₂	143.9[1.9] → Col _{ro2} (P2m) ← 152.7[60.3] → I.L.
1e : (<i>m</i> -C ₈ OPhS) ₈ PcCu			K _{1v}	106.5 → Col _{ro2} (P2m) ← 142.6[60.3] → I.L.
			K _{2v}	100.1 → Col _{ro2} (P2m) ←
			K _{3v}	96.3 → Col _{ro2} (P2m) ←
1f : (<i>m</i> -C ₁₀ OPhS) ₈ PcCu	K ₁	41.6[7.3]	K _{2v}	64.7[3.2] → Col _{ro1} (P2m) ← 81.1[7.5] → Col _{ro2} (P2m) ← 133.5[95.5] → I.L.
				58.6[18.1] ← Col _{ro1} (P2m) →
1g : (<i>m</i> -C ₁₂ OPhS) ₈ PcCu			K ₁	81.5 → Col _{ro1} (P2m) ← 98.5 → Col _{ro2} (P2m) ← 110.9[67.0] → I.L.
			Col _{ro1} (P2m)	55.0 → Col _{ro2} (P2m) ←
1h : (<i>m</i> -C ₁₄ OPhS) ₈ PcCu			Col _{ro2} (P2m)	38.1 [4.1] → Col _{ro1} (P2m) ← 93.2[6.5] → Col _{ro2} (P2m) ← 117.9[70.9] → I.L.
			K _{1v}	63.9 → Col _{ro1} (P2m) ←
1i : (<i>m</i> -C ₁₆ OPhS) ₈ PcCu			K _{1v}	75.0 → Col _{ro} (P2m) ← 111.2[48.9] → I.L.
			K _{2v}	64.0 → Col _{ro} (P2m) ←

Phase nomenclature: K = crystal, Col_{ro} = rectangular ordered columnar, I.L. = isotropic liquid and v = virgin state. Col_{ro1}~Col_{ro2}: See Figure 2. * Ref [20].

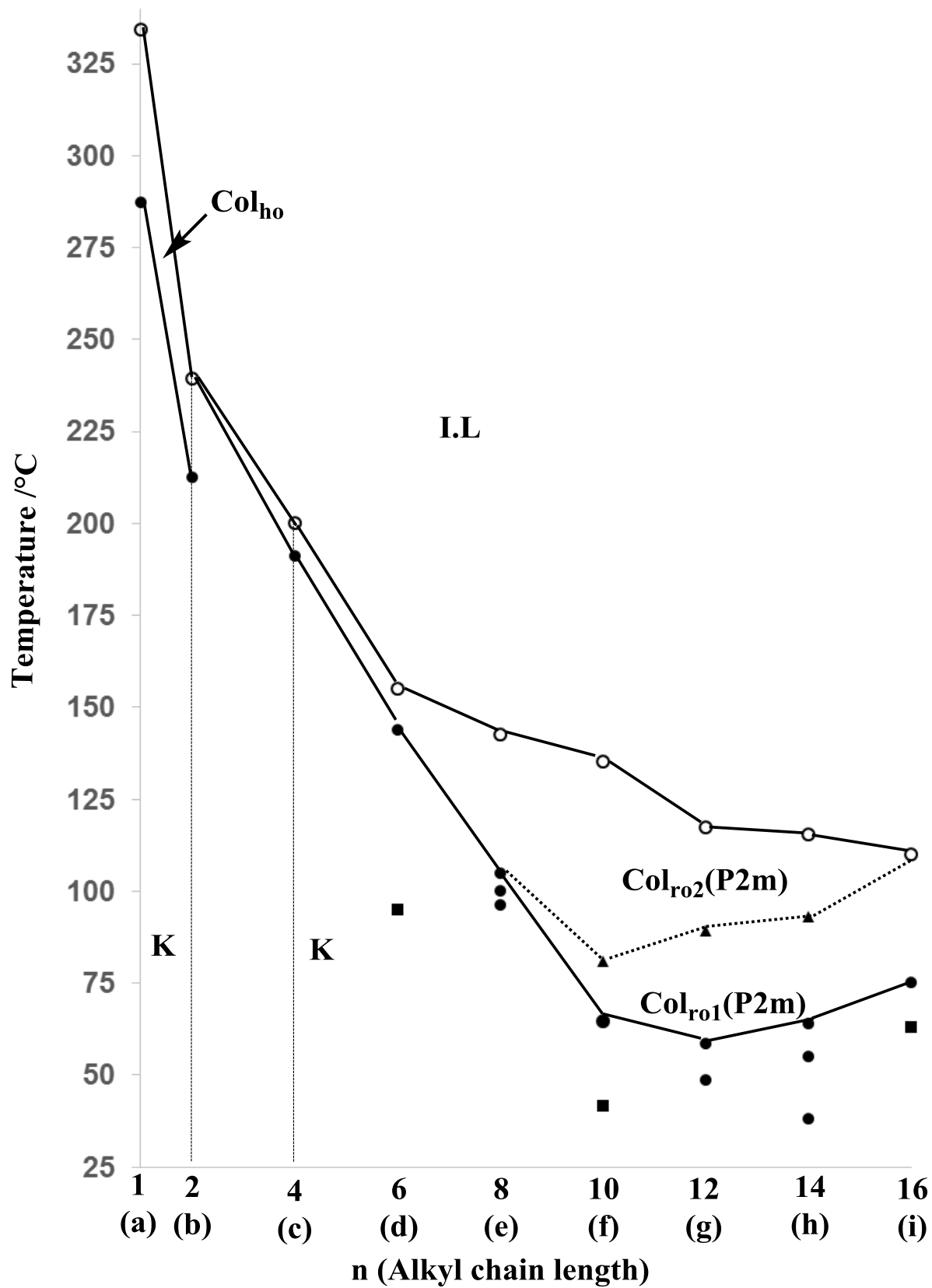


Fig. 2. Phase transition temperature versus the number of carbon atom in the alkoxy chains for $(m-C_nOPhS)_8PcCu$ (1a-i). \circ : clearing point, \bullet : melting point, \blacksquare : crystal-crystal phase transition, and \blacktriangle : mesophase-mesophase transition.

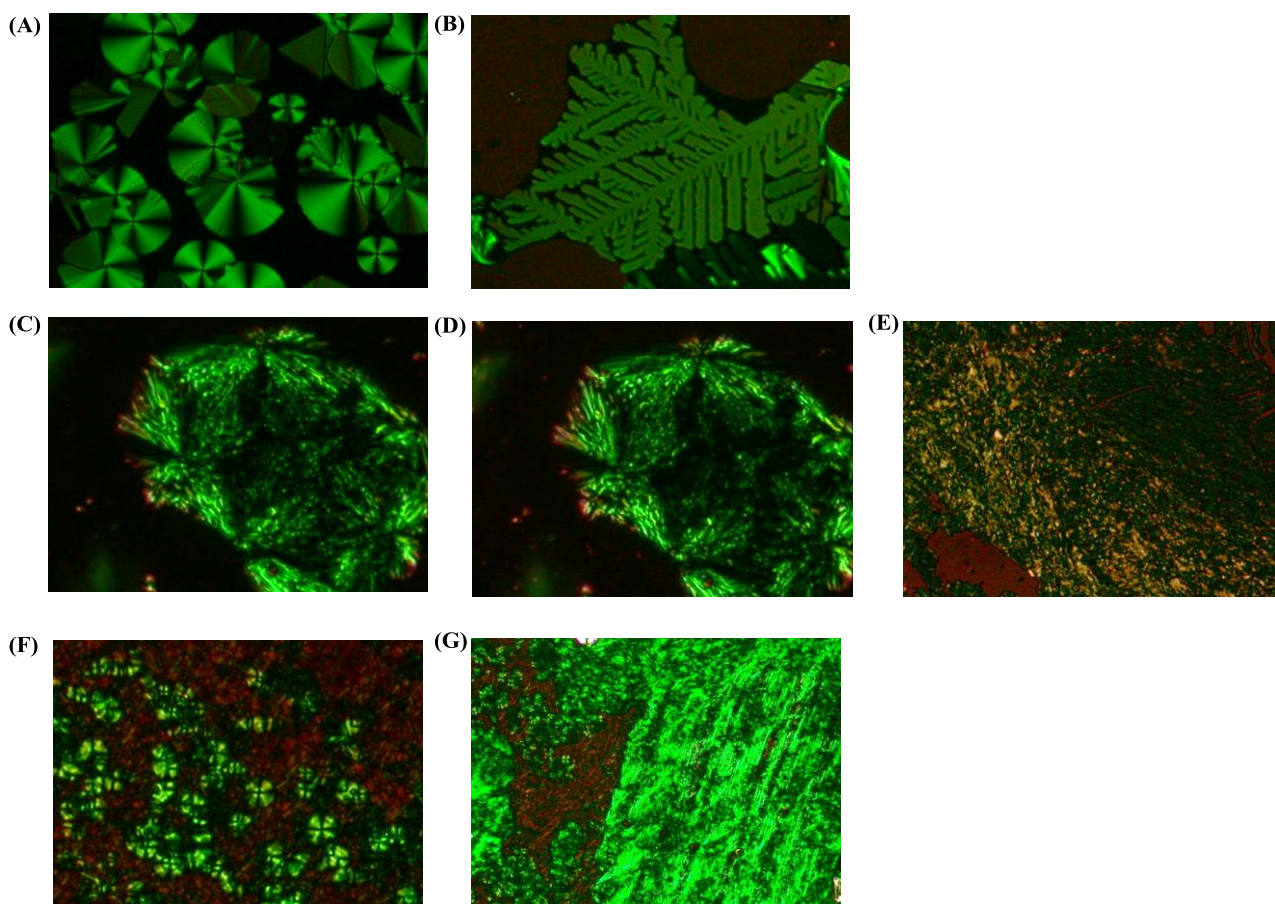


Fig. 3. Photomicrographs of (A) and (B): Col_{h0} of (*m*-C₂OPhS)₈PcCu (**1b**) at 220 °C; (C) Col_{r02}(P2m) of (*m*-C₁₀OPhS)₈PcCu (**1f**) at 115 °C; (D) Col_{r01}(P2m) of (*m*-C₁₀OPhS)₈PcCu (**1f**) at 90 °C; (E) sheared sample of the photo (D) of **1f** at 90 °C; (F) Col_{r01}(P2m) of (*m*-C₁₆OPhS)₈PcCu (**1i**) at 100 °C; (G) sheared sample of the photo (F) of **1i** at 100 °C.

Table 4. X-ray data of 1a~i.

Compound (mesophase)	Lattice constants/Å	Spacing/Å		Miller indices	
		Observed	Calculated	(hkl)	
1a* : (<i>m</i> -C ₁ OPhS) ₈ PcCu Col _{h0} at 300°C	a = 20.9 h = 6.82 Z = 0.95 for ρ = 1.1	18.1	18.2	(100)	
		13.6	13.6	(001) ^{2h}	
		10.1	10.5	(110)	
		9.16	9.05	(200)	
		6.82	6.82	(001) ^h	
		ca.5.9	6.03	(300)+#1	
		3.98	3.95	(410)	
		1b : (<i>m</i> -C ₂ OPhS) ₈ PcCu Col _{h0} at 220°C	a = 22.0 h = 7.12 Z = 1.0 for ρ = 1.1	19.0	19.0
14.3	14.4			(001) ^{2h}	
10.9	11.0			(110)	
7.12	7.19			(210)+(001) ^h	
6.23	6.34			(300)	
ca.5.2	-			#1	
4.00	4.15			(410)	
1c : (<i>m</i> -C ₄ OPhS) ₈ PcCu Col _{ro2} (P2m) at 199°C	a = 22.7 b = 21.7 h = 7.17 Z = 1.1 for ρ = 1.0			22.7	22.7
		10.8	10.8	(020)	
		7.17	7.17	(001) ^h	
		5.26	5.27	(140)	
		4.88	4.89	(240)+#1	
		4.18	4.19	(520)	
		3.71	3.73	(610)	
		1d : (<i>m</i> -C ₆ OPhS) ₈ PcCu Col _{ro2} (P2m) at 148°C	a = 36.8 b = 26.6 h = 3.60 Z = 1.0 for ρ = 1.1	26.6	26.6
18.4	18.4			(200)	
10.7	10.8			(220)	
8.61	8.63			(130)	
7.92	8.00			(230)	
5.82	5.85			(340)	
5.02	5.04			(630)	
4.58	4.60			(800)+#2	
4.06	4.08			(830)	
3.60	3.60			(001) ^h	
1e : (<i>m</i> -C ₈ OPhS) ₈ PcCu Col _{ro2} (P2m) at 115°C	a = 35.0 b = 27.5 h = 3.99 Z = 1.0 for ρ = 1.1	35.0	35.0	(100)	
		21.6	21.6	(110)	
		15.9	14.8	(210)	
		10.8	10.7	(310)	
		7.06	7.00	(500)	
		6.58	6.41	(240)	
		5.14	5.25	(250)+#2	
		4.69	4.70	(720)+#2	
		3.99	3.99	(001) ^h	
		1f : (<i>m</i> -C ₁₀ OPhS) ₈ PcCu	Col _{ro1} (P2m) at 80°C	a = 36.6 b = 27.2 h = 4.01 Z = 0.98 for ρ = 1.1	36.6
21.8	21.8				(110)
13.7	13.6				(020)
10.7	10.9				(220)
6.93	7.07				(510)
5.01	4.98				(540)+#2
4.61	4.57				(800)+#2
4.01	4.01				(001) ^h
Col _{ro2} (P2m) at 115°C	a = 37.0 b = 27.6 h = 4.06 Z = 1.0 for ρ = 1.1		37.0	37.0	(100)
			22.1	22.1	(110)
			10.6	11.1	(220)
			7.06	7.15	(510)
			5.08	5.05	(540)+#2
			4.61	4.60	(060)+#2
			4.06	4.06	(001) ^h

Table 4 . (continued.)

Compound (mesophase)	Lattice constants/Å	Spacing/Å		Miller indices (<i>hkl</i>)
		Observed	Calculated	
1g : (<i>m</i>-C₁₂OPhS)₈PcCu				
Col _{ro2} (P2m) at 100°C	a = 39.5	39.5	39.5	(100)
	b = 21.3	21.3	21.3	(010)
	<i>h</i> = 5.09	10.7	10.7	(020)
	Z = 0.97 for ρ = 1.1	8.02	7.90	(500)
		6.98	7.00	(130)
		5.09	5.09	(001) ^h
		4.63	-	#2
Col _{ro1} (P2m) at 90°C	a = 43.1	43.1	43.1	(100)
	b = 21.6	21.6	21.6	(010)
	<i>h</i> = 4.96	13.7	13.7	(300)
	Z = 1.1 for ρ = 1.1	10.8	10.8	(400)
		7.04	7.11	(130)
		4.96	4.96	(001) ^h
		4.62	-	#2
1h : (<i>m</i>-C₁₄OPhS)₈PcCu				
Col _{ro2} (P2m) at 105°C	a = 43.7	43.7	43.7	(100)
	b = 21.5	21.5	21.5	(010)
	<i>h</i> = 5.08	14.4	14.6	(300)
	Z = 1.0 for ρ = 1.1	10.6	10.7	(020)
		7.14	7.15	(030)
		5.08	5.08	(001) ^h
		ca.4.6	-	#2
Col _{ro1} (P2m) at 85°C	a = 50.1	50.1	50.1	(100)
	b = 22.6	22.6	22.6	(010)
	<i>h</i> = 4.59	14.3	13.4	(310)
	Z = 1.1 for ρ = 1.1	10.7	11.0	(410)
		7.09	7.16	(700)
		ca.4.9	-	#2
		4.59	4.59	(001) ^h
1i : (<i>m</i>-C₁₆OPhS)₈PcCu				
Col _{ro1} (P2m) at 100°C	a = 49.9	49.9	49.9	(100)
	b = 28.6	24.8	24.8	(110)
	<i>h</i> = 4.07	17.0	16.6	(300)
	Z = 1.0 for ρ = 1.0	10.7	10.8	(320)
		7.07	7.07	(140)
		ca.5.1	-	#2
		ca.4.6	-	#2
4.07	4.07	(001) ^h		

#1, #2 = Broad halos due to the thermal fluctuation of the phenylthio groups and the molten alkyl chains, respectively. *h* = Stacking distance. ρ = assumed density (g/cm³). * Ref [20].

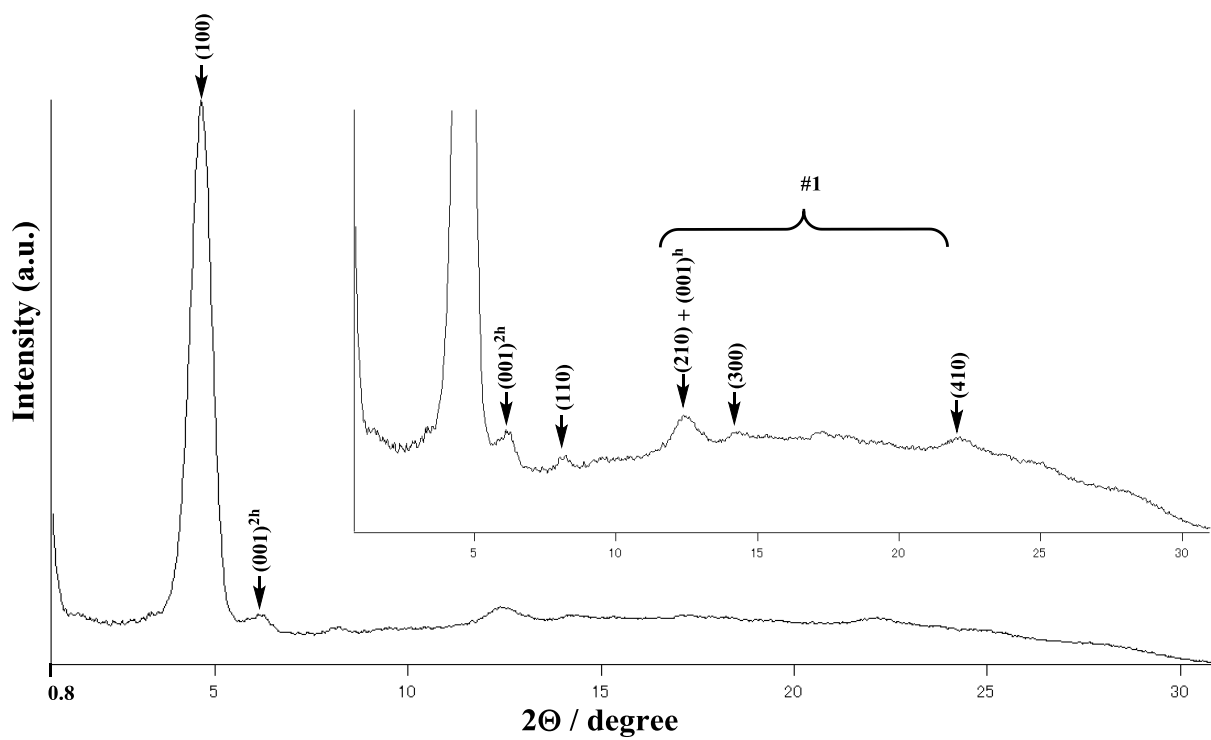


Fig. 4. XRD pattern of $(m\text{-C}_2\text{OPhS})_8\text{PcCu}$ (**1b**) at $220\text{ }^\circ\text{C}$ (on cooling from I.L). #1 = Broad halo due to the thermal fluctuation of the phenylthio groups.

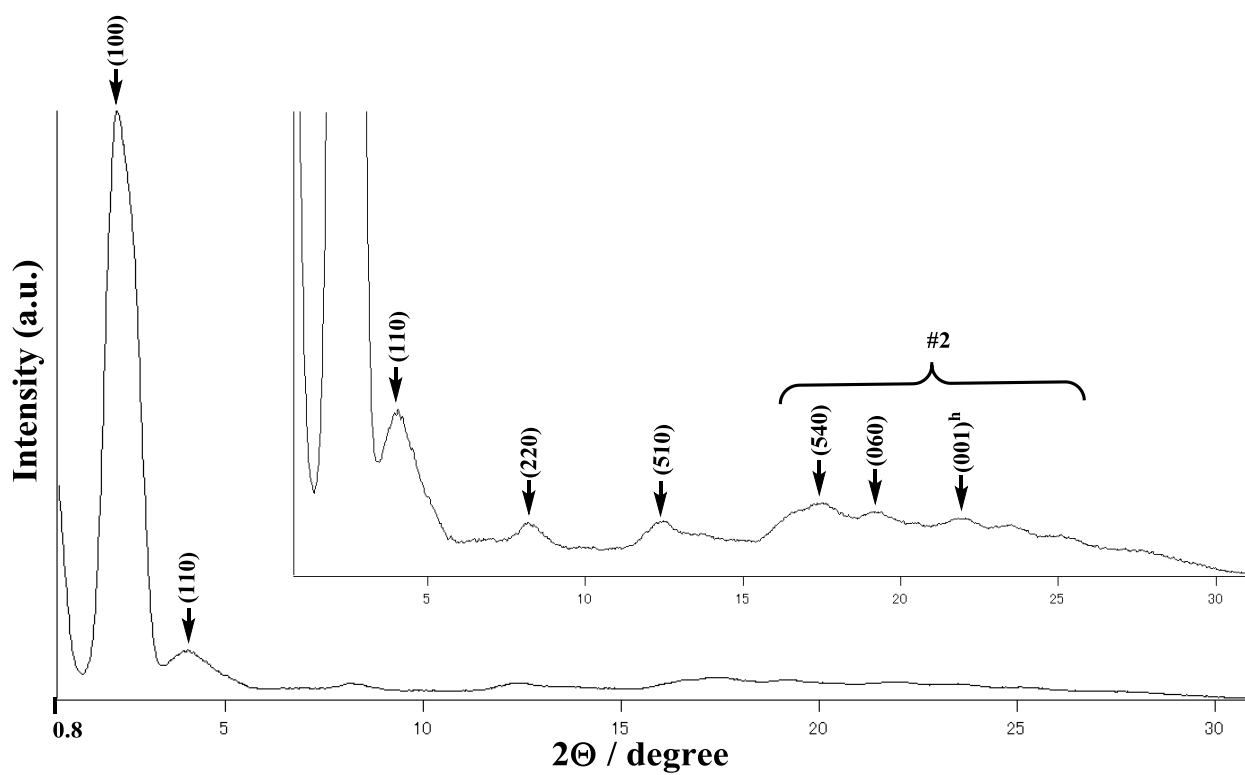


Fig. 5. XRD pattern of $(m\text{-C}_{10}\text{OPhS})_8\text{PcCu}$ (**1f**) at $115\text{ }^\circ\text{C}$. #2 = Broad halo due to the molten alkyl chains.

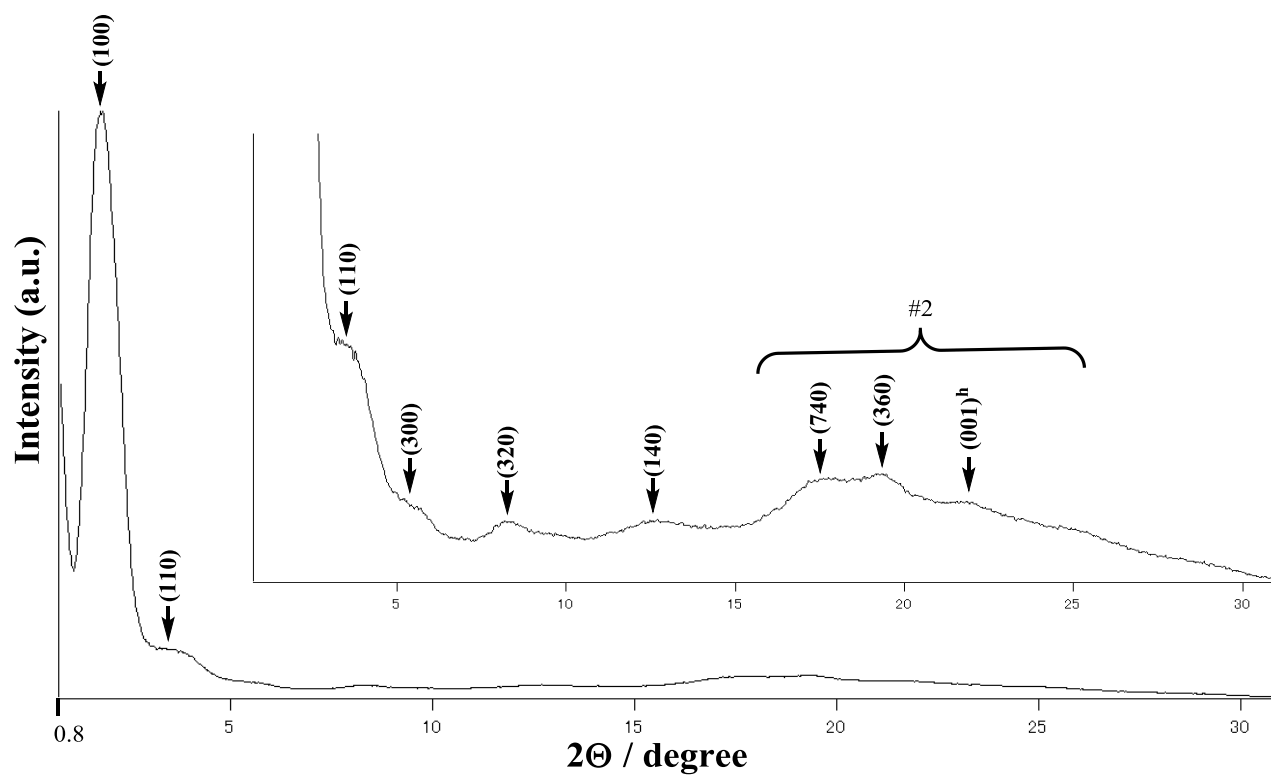
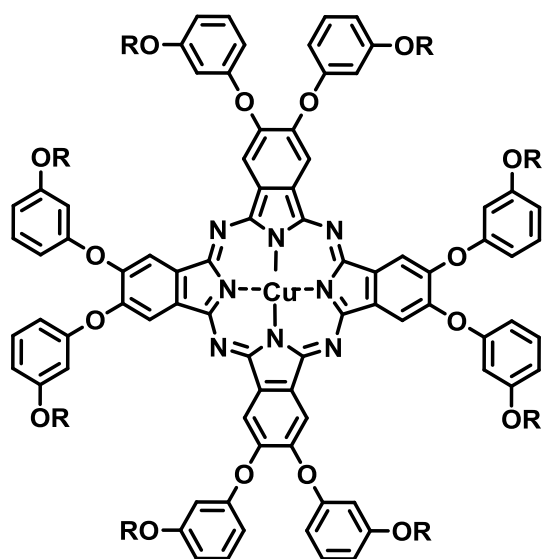
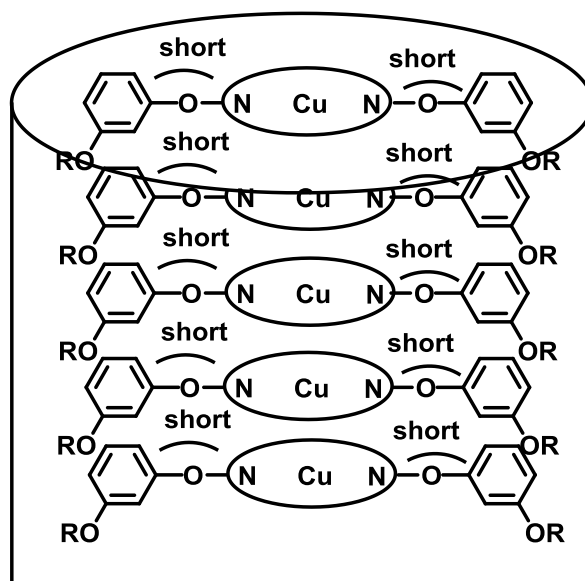


Fig. 6. XRD pattern of $(m\text{-C}_{16}\text{OPhS})_8\text{PcCu}$ (1i) at 100 °C (on cooling from I.L). #2 = Broad halo due to the molten alkyl chains.

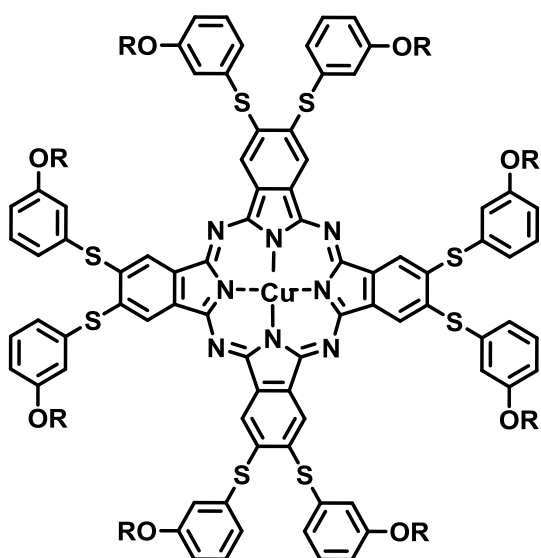
$(m\text{-C}_n\text{OPhO})_8\text{PcCu}$ ($n = 10\text{-}20$)



Col_{ho}



$(m\text{-C}_n\text{OPhS})_8\text{PcCu}$ ($n = 4\text{-}16$)



$\text{Col}_{\text{ro}}(\text{P2m})$

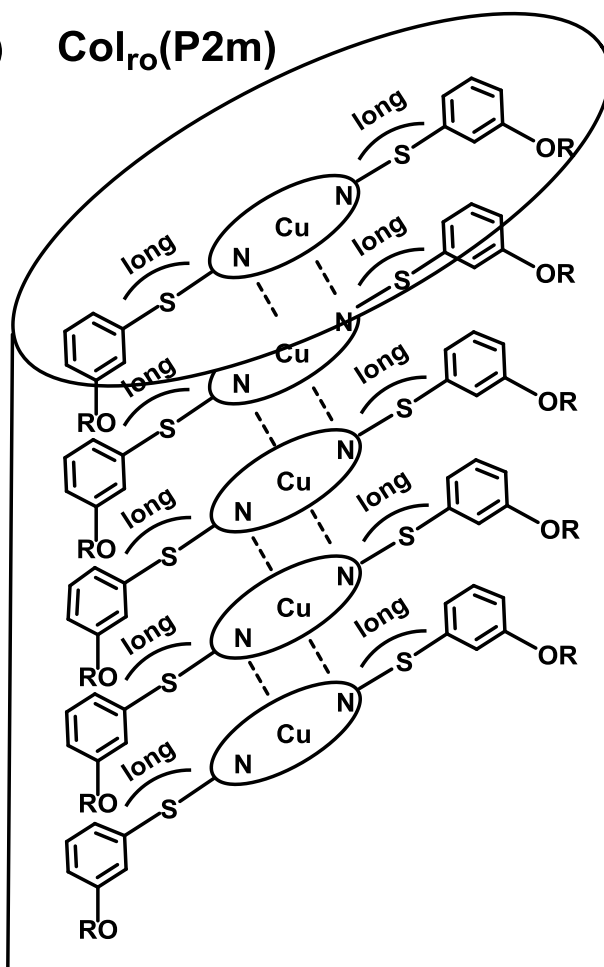


Fig. 7. Columnar stacking structures of $(m\text{-C}_n\text{OPhO})_8\text{PcCu}$ ($n = 10\text{-}20$) and $(m\text{-C}_n\text{OPhS})_8\text{PcCu}$ ($n = 4\text{-}16$).

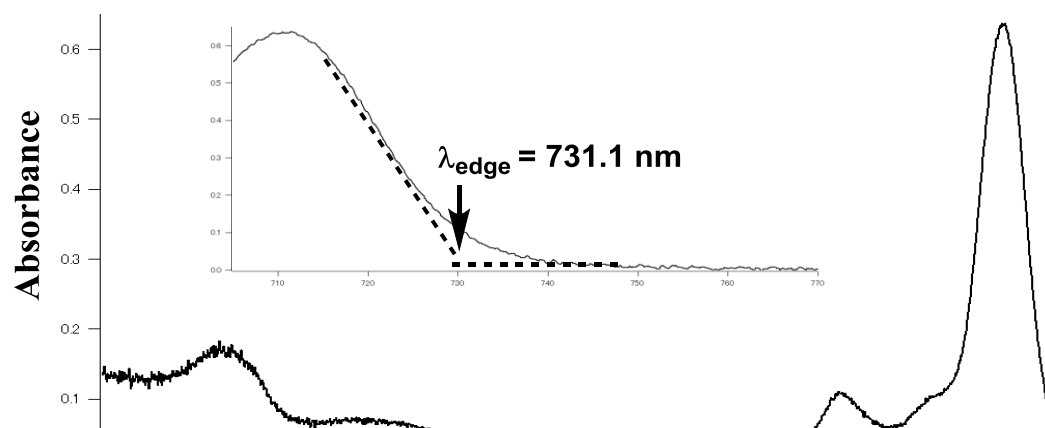
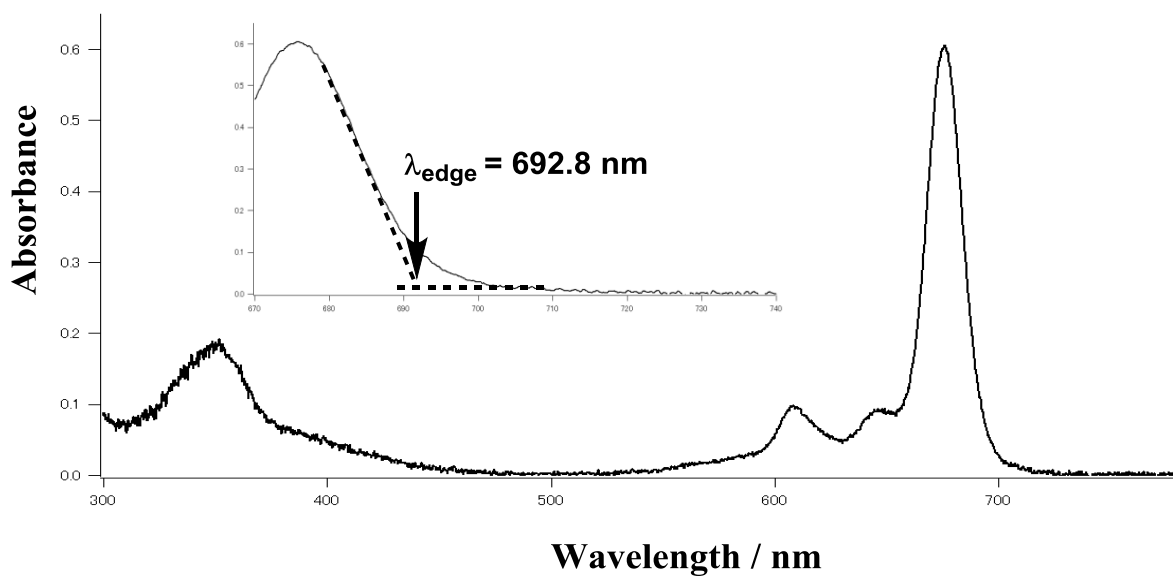


Fig. 8. UV-vis absorption spectra of $(m\text{-C}_{10}\text{OPhO})_8\text{PcCu}$ (upper) and $(m\text{-C}_{10}\text{OPhS})_8\text{PcCu}$ (**1f**) (lower) in THF solution.

Table 5. UV-vis spectral data of (*m*-C₁₀OPhO)₈PcCu and (*m*-C₁₀OPhS)₈PcCu in THF solution.

Compound	Concentration ($\times 10^{-6}$ mol L ⁻¹)	$\lambda_{\text{abs}} / \text{nm}$ (log ϵ)			λ_{edge} / nm	$E_{\text{gap}}^* / \text{eV}$
		Soret band	Q-band			
			Q ₀₋₁ -band	Q ₀₋₀ -band		
(<i>m</i> -C ₁₀ OPhO) ₈ PcCu	2.27	351.9(4.93)	608.3(4.64)	675.9(5.43)	692.8	1.79
(<i>m</i> -C ₁₀ OPhS) ₈ PcCu (1f)	2.29	353.3(4.90)	635.7(4.69)	711.6(5.44)	731.1	1.70

* E_{gap} was estimated from the absorption edge of Q-band.